# TARGETING RESPIRATORY SYNCYTIAL VIRUS USING PEPTIDE MIMETICS

# TARGETING RESPIRATORY SYNCYTIAL VIRUS USING A CHIMERIC PHOSPHOPROTEIN MIMETIC

By JORDAN C. NELSON, B.Sc.

A Thesis Submitted to the School of Graduate Studies in Partial Fulfillment of the Requirements for the Degree Master of Science

# DESCRIPTIVE NOTE

McMaster University, MASTER OF SCIENCE (2015) Hamilton, Ontario (Medical Sciences)

TITLE: Inhibition of Respiratory Syncytial Virus Using a Chimeric Phosphoprotein Mimetic

AUTHOR: Jordan C. Nelson,B.Sc. (Life Science, McMaster University)

SUPERVISOR: Dr. James Mahony

NUMBER OF PAGES: xvi, 109

# ABSTRACT

Respiratory syncytial virus (RSV) is a pathogen associated with lower respiratory tract infection, and is a common cause of infant hospitalization worldwide. Despite efforts to create safe and cost-effective RSV therapeutics, there remains no vaccine, and antiviral drugs have been developed with limited success. Among the 11 proteins coded by the negative-sense single-stranded RNA genome of RSV, the phosphoprotein (P) and nucleoprotein (N) aid in the formation of an RNA-dependent RNA polymerase (RdRp) complex, which is essential for RSV virulence. The specificities of the N-P binding interaction have been researched extensively, which has provided researchers with a novel target for an RSV therapeutic. In this study, a recombinant peptide mimetic ($P_{220-241}$) containing the final 21 C-terminal amino acids of RSV P fused to Maltose-Binding Protein (MBP), and a cell-penetrating peptide (CPP), was purified for the purpose of targeting this interaction. In addition to successfully entering cells, the peptide was shown to inhibit both RSV subtype A and subtype B infection *in vitro*, with a percent inhibition (PI) of infection as high as 95% at 20 μM. Additionally, $P_{220-241}$ did not inhibit infection of parainfluenza virus type 2 (PIV-2), indicating this inhibition was not an artifact of the peptide acting as a pathogen-associated molecular pattern (PAMP). A series of three different assays demonstrated that $P_{220-241}$ does not appear to have any cytotoxic effects *in vitro*. Finally, using both glutathione S-transferase (GST) pull-downs and *in vitro* immunoprecipitations, we demonstrated that $P_{220-241}$ is able to bind the N protein, while also preventing binding of full-length P protein. Taken together, this study provides the framework for a novel method of targeting RSV protein-protein interactions using chimeric cell-penetrating peptide mimetics.

# ACKNOWLEDGEMENTS

Firstly, I would like to thank my supervisor, Dr. James Mahony, for giving me the opportunity to conduct exciting and innovative research in his laboratory. Over my two years in the program I have learned a great deal under his supervision, and I was very much inspired by his passion and enthusiasm for research in general. My research experience prior to my Masters was minimal, and his patience and assistance throughout my project was much appreciated. I consider myself very fortunate to have learned from a researcher who has such a dedication towards his students, and I look forward to using his tutelage as I move forward in my academic career. Furthermore, I would like to thank my committee members, Dr. Marie Elliot and Dr. Murray Junop, for their continuous support and guidance throughout the duration of my project. Coming from different fields of research, they were both able to provide me with unique perspectives, and both continuously challenged me as I progressed on my project. A special thanks as well to Dr. Junop for remaining on my committee and supporting my research project even after moving to Western University.

I am honoured to have spent these two years working with so many dedicated and intelligent students in the Mahony laboratory. Dr. Christopher Stone has been a great mentor throughout my project both in the laboratory, and on the golf course. While it is difficult to admit, David Bulir's passion and dedication towards sound scientific research was very admirable. David was an amazing teacher and continuously pushed both myself and the other lab members to get the very most out of our projects. I would also like to thank all the other lab members who helped make this experience as

enjoyable as it was: Sylvia Chong, Steven (Shu) Liang, Christopher Chiang, Kenneth Mwawasi, Samantha Mihalco, Zachariah Scinocca, and Steven Zhiang.

I owe my deepest gratitude to my family and friends who have provided support and encouragement throughout the duration of my Masters. My roommates from 150 Arkell street helped make my time at McMaster as enjoyable as possible. Most importantly, I would like to thank my brother, David, and parents, Karen and Chris. They were a continuous source of inspiration and motivation throughout both my undergraduate and graduate studies at McMaster. I could not have made it to this point without their support, and I hope that upon completion of my thesis I will have made them proud.

*This thesis is dedicated to my mother and father, Karen and Chris Nelson.*

# TABLE OF CONTENTS

# List of Abbreviations

**ABD –** Albumin-Binding Domain

**ALRI** – Acute lower respiratory tract infection

**AMR** – ATP monitoring reagent

**BRSV** – Bovine respiratory syncytial virus

**BSA** – Bovine serum albumin

**CH** – Cycloheximide

**CTL** – Cytotoxic T lymphocyte

**DARPin** – Designed Ankyrin Repeat Protein

**DFA** – Direct fluorescent assay

**DMEM** – Dulbecco's Modified Eagle Medium

**EDTA** – Ethylenediaminetetraacetic acid

**E. coli** – Escherichia. coli

**ELISA** – Enzyme-linked immunosorbent assay

**FBS** – Fetal bovine serum

**FOV** – Field of view

**F** – Fusion protein

**FDA** – Food and Drug Administration

**FI** – Formalin-innactivated

**FITC** – Fluorescein isothiocyanate

**FPLC** – Fast protein liquid chromatography

**GAG** – Glycosaminoglycan

**GE** – Gene-end sequence

**G** – Glycoprotein

**GS** – Gene-start sequence

**GST** – Glutathione S-transferase

**GTP** – Guanosine-5'-triphosphate

**HBD** – Heparin Binding Domain

**HeLa** – Henrietta Lacks cell line

**HIV-1** – Human immunodeficiency virus type 1

**HRP** – Horseradish peroxidase

**HSA** – Human serum albumin

**IB** – Inclusion body

**IgG** – Immunoglobulin G

**IFN-β** – Interferon-beta

**IMPDH** – Inosine monophosphate dehydrogenase

**IPTG** – Isopropyl β-D-thiogalactopyranoside

**ITC** – Isothermal titration calorimetry

**$K_D$** – Dissociation constant

**LB** – Luria Bertani broth

**LDAO** – N,N-dimethyldodecylamine N-oxide

**Le** – Leader sequence

**L** – Large polymerase

**LTCF** – Long-term care facility

**MAb** – Monoclonal antibody

**MBP** – Maltose-Binding Protein

**M/M2-1/M2-2** – Matrix proteins 1/2

**MeV** – Measles virus

**mFc** – Monoclonal Fc domain

**MuV** – Mumps virus

**N** – Nucleoprotein

**N°** – Nucleoprotein (newly synthesized)

**NDV** – Newcastle disease virus

**NiV** – Nipah virus

**NS1/NS2** – Non –structural proteins

**OD** – Optical density

**PAMP** – Pathogen-associated molecular pattern

**PB1** – Polymerase Basic Protein 1

**PBS** – Phosphate buffered saline

**PBST** – Phosphate buffered saline with 0.1% Tween-20

**PCR** – Polymerase chain reaction

**PI** – Percent inhibition

**PICU** – Pediatric intensive care unit

**PIV-2** – Parainfluenza virus type 2

**$P_{220-241}$** – Phosphoprotein mimetic peptide

**P** – Phosphoprotein

**RdRp** – RNA-dependent RNA polymerase complex

**RFU** – Relative fluorescence unit

**RNAi** – RNA interference

**RPM** – Revolutions per minute

**RSV** – Respiratory syncytial virus

**RT-PCR** – Reverse-transcription polymerase chain reaction

**SDS-PAGE** – Sodium dodecyl sulfate polyacrylamide gel electrophoresis

**SH** – Small hydrophobic protein

**siRNA** – Small interfering ribonucleic acid

**Smac** – Second mitochondria derived activator of capsase

**SPR** – Surface plasmon resonance

**TEMED** – Tetramethylethylenediamine

**TNF-α** – Tumor Necrosis Factor Alpha

**Tr** – Trailer sequence

**T6E** – Threonine to glutamic acid substitution

**V –** Volts

**W** – Watts

**x g** – Centrifugal force

# LIST OF FIGURES

# LIST OF TABLES

# DECLARATION OF ACADEMIC ACHIEVEMENT

Jordan C. Nelson performed all of the experiments described in this thesis with the exception of the following:

1. Cloning of the original $P_{220\text{-}241}$ construct was performed by David Bulir.
2. The PrestoBlue BEAS-2B cell replication assay in **Supplementary Figure S2** was performed by Christopher Chiang.

# CHAPTER ONE

# INTRODUCTION

## 1.1 Overview and history of RSV

Human respiratory syncytial virus (RSV) is a common pathogen associated with acute lower respiratory tract infection (ALRI) (Nair et al, 2011). Originally isolated in 1966 from a colony of chimpanzees showing symptoms of coryza, and labeled as “chimpanzee coryza agent”, RSV frequently manifests itself as bronchiolitis or pneumonia, and in severe cases can lead to death (Blount et al, 1956; Hall, 2001). The term “syncytium” is of Greek origin, and refers to the unique ability of RSV to cause the cell membranes of nearby cells to fuse, thus forming multiple syncytia (see **Figure 1.1**) (Pastey et al, 1999). RSV is negative-sense single-stranded RNA virus, and a member of the *Paramyxoviridae* family (Collins et al, 1996). There are two main genera of RSV, RSV A and RSV B, which are further divided into additional subtypes (McConnochie et al, 1990). To date, no animal reservoir has been discovered for RSV (Martinez et al, 2009). Persistence of the virus in humans is thought to help maintain RSV strains in between epidemics (Martinez et al, 1990). These outbreaks seem to display a seasonal trend in certain regions. For example, there is a noticeable winter peak of RSV-associated hospitalizations in the United States, while in many tropical regions RSV remains prevalent year-round (Panozzo et al, 2007; Stenballe et al, 2012).

RSV most commonly infects children at a very young age, with the majority being affected prior to the age of two (Paes et al, 2011). In fact, RSV is

the most common cause of infant hospitalization worldwide, with children less than a year of age having a hospitalization rate of approximately 2.35% (Zhou et al, 2012). Of those children hospitalized for RSV-related infections, 50% to 90% will develop bronchiolitis (Paes et al, 2011). In adults, RSV infection is typically mild, manifesting itself as a common cold, while in infants the symptoms are frequently much more severe (La Via et al, 1992). Clinically, infants typically present with coryza, throat congestion, and a fever (La Via et al, 1992). After a short incubation period of 2 to 5 days, more severe symptoms may develop, including wheezing and shortness of breath (La Via et al, 1992). While the majority of cases are treated successfully, up to 199,000 deaths in children below the age of five can be attributed to RSV infection (Nair et al, 2010). RSV thus presents a substantial global economic burden. For example, the total annual medical costs for RSV-related hospitalizations of children were estimated at $652 million in the United States alone (Paramore et al, 2004).

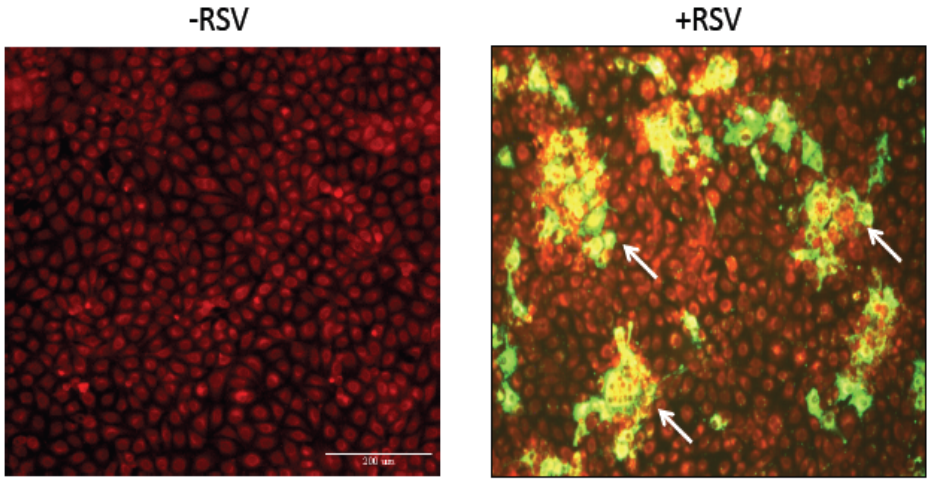


**Figure 1.1 RSV syncytium formation**
Infection with RSV results in distinct formation of cellular syncytia (right panel). This process is mediated by the outer F protein of RSV. The above figure represents LLC-MK2 cells which were either uninfected (left panel), or infected with RSV (right panel) for 48 hours. The cells were visualized with fluorescence microscopy with RSV-infected cells stained green (FITC) and uninfected cells stained red (Evan's blue). White arrows represent the formation of distinct cellular syncytia.

## 1.2 Taxonomy and nomenclature

RSV is a member of the *Paramyxoviridae* family of viruses (also known as paramyxoviruses), which is from the *Mononegavirales* order (Chang et al, 2012; Collins et al, 2011). This family includes several lipid-encapsulated negative-sense single-stranded RNA viruses, such as mumps virus (MuV), measles virus (MeV), parainfluenza virus (PIV), and nipah virus (NiV) (Chang et al, 2012). Certain paramyxoviruses are also capable of infecting other species, such as Newcastle disease virus (NDV) and bovine respiratory syncytial virus (BRSV) (Chang et al, 2012). While these viruses contain similar features to those within the *Orthomyxoviridae* family, their RNA genome is monopartite (non-segmented) in nature (Mayo, 1995). Additionally, while the genomes of paramyxoviruses code

for one or more nucleocapsid, phosphoprotein, matrix, fusion, glycoprotein, non-structural, and polymerase proteins, there remain unique aspects in each of their respective life cycles (Chang et al, 2012; Samal, 2011). The paramyxovirus family consists of two subfamilies, *Paramyxovirinae*, which includes 5 genera, and *Pneumovirinae*, which includes two genera (Chang et al, 2012). RSV is member of the *Pneumovirus* genus, from the *Pneumovirinae* subfamily (Chang et al, 2012; Yu et al, 1991). The paramyxoviruses are divided into these seven genera based on several criteria, including distinguishing features in their viral attachment proteins, relative gene orders, morphologic criteria, and sequence homology (Chang et al, 2012; Enders, 1991). For example, while the parainfluenza virus attachment proteins contain both neuraminidase and hemagglutinating activity, RSV lacks both these features (Enders, 1991).

The development of monoclonal antibody (MAb) technologies initially helped uncover that RSV naturally occurs as one of two distinct antigenic subtypes, A or B (Mufson et al, 1985; Sullender, 2010; Walsh and Hruska, 1983). Cloning of RSV cDNA and nucleotide sequencing confirmed that the outer glycoprotein (G) contains the greatest amount of antigenic variation, with a 47% difference in amino acid sequences (Sullender, 2010). The major antigenic subtypes can be further divided into different strains. However, the amino acid differences between these strains are rather negligible compared to the major subtypes. For example, there is only a 6% difference in amino acid sequences between the Long and A2 strains from the group A subtype (Sullender, 2010).

There remains a significant gap in knowledge concerning the contribution of these two subtypes towards both disease severity, and yearly outbreaks. Early epidemiological studies were suggestive of a dominance of group A RSV strains during outbreaks (approximately 60% RSV A versus 40% RSV B) (Hendry et al, 1989). However, both subtypes have been shown to circulate concurrently, or alternate in dominance during outbreaks (Coates et al, 1966; Hendry et al, 1989; Wright and Piedimonte, 2011). Lastly, several published studies suggest RSV A-induced infection appears to be much more severe than that of the related RSV B subtype; however this topic remains controversial (McConnochie et al, 1990; Papadopoulos et al, 2004). RSV A isolates have been shown to replicate faster, thereby producing higher titers in both cell culture and animal models (Sullender, 2010).

## 1.3 Clinical presentation and epidemiology

As previously described, RSV is most well known for its ability to infect infants during their first few years of life, however the elderly, as well as individuals with compromised immune, pulmonary, or cardiac function are also susceptible to RSV infection (Hall et al, 2013; La Via et al, 1992). The seroprevalence of RSV is approximately 71% in individuals between the ages of 2 and 9, and 95% between the ages of 10 and 69 (Sastre et al, 2012). RSV has several common modes of transmission. These include contact with the nose or

eyes in the form of large particle aerosols, and also by direct contact with large droplets or fomites from the hands or nose (Hall et al, 2001). The ability of RSV to survive for prolonged periods of time on ones skin and other surfaces helps enhance transmission, especially nosocomial spread (Hall et al, 2001).

There is a wide range of symptoms associated with RSV infection, which depend primarily on the patient's age, health status, and also if the patient was previously infected with the virus (Borchers et al, 2013; Hall et al, 2013). Primary infection with RSV is almost always symptomatic (Borchers et al, 2013). Typically, RSV infection begins in the epithelial cells of the nasopharynx, with individuals presenting common symptoms such as a mild fever, coryza, and congestion (Borchers et al, 2013; La Via et al, 1992). While in many patients symptoms will begin to subside after 2 to 3 days, in more severe cases, infectious RSV virions often enter the lower respiratory tract (Borchers et al, 2013; La Via et al, 1992). This typically occurs after an incubation period of 2 to 5 days, and includes symptoms such dyspnea and wheezing (La Via et al, 1992). In individuals suffering from these severe cases of lower respiratory tract infection (15% to 20% of infants), the illness most frequently presents itself as bronchiolitis, however pneumonia is also common (Borchers et al, 2013; La Via et al, 1992). Infection of the bronchiolar epithelium is characterized by epithelial cell necrosis, mucus hypersecretion, as well as infiltrates of macrophages, plasma cells, and lymphocytes into the peribronchiolar space (La Via et al, 1992). The result is a dense buildup of mucus and cellular debris, thus predisposing

patients to airway obstruction (La Via et al, 1992). Re-infections with RSV are not uncommon. In fact, infants who become infected with RSV within their first 12 months of life have a re-infection rate of approximately 30% to 75% (Borchers et al, 2013). Alternatively, re-infections that occur in older children or adolescents are typically mild to moderate in severity, and rarely migrate to the lower respiratory tract (Borchers et al, 2013; Walsh and Falsey, 2012). Additionally, while deaths from RSV infection are rare, mortality rates are substantially higher in under developed countries (Nair et al, 2010).

While a major focus of RSV research resides around preventing infection in infants, several other important groups are beginning to garner increased attention. Previous research estimates that RSV infection is responsible for approximately 10,000 deaths annually of persons over the age of 65 in the United States alone (Falsey et al, 2005; Thomson et al, 2003). Even though RSV was initially discovered in the 1950s, it was not until several nursing home outbreaks in the 1980s that RSV was declared a serious pathogen in the elderly population (Falsey and Walsh, 2000). RSV research involving this age group remains relatively scarce, however previous reports suggest rates of RSV-induced pneumonia could be as high as 55%, and most of these studies involved elderly individuals in long-term care facilities (LTCF) (Falsey and Walsh, 2000). While the main symptoms that present in elderly patients are similar to those seen infants, treating these individuals is often more difficult due to other complicating health issues (Falsey and Walsh, 2000). Several other groups of individuals are

also known to be predisposed for RSV infection due to certain health complications. These include prematurely born infants, individuals with chronic lung disease of prematurity, immune deficiencies, and congenital heart disease (Welliver, 2003). When suffering from RSV infections, these patients often present with more severe symptoms and consequently have higher death rates (Welliver, 2003). Prematurely born infants, as well as those born with chronic lung disease often have underdeveloped airways of below average diameter, making them much more susceptible to inflammatory reactions caused by RSV-induced bronchiolitis and pneumonia (Welliver, 2003). Individuals with congenital heart disease on average have longer hospital stays and an increased occurrence of respiratory failure (Welliver, 2003). Lastly, immunocompromised patients by virtue of steroids, cancer chemotherapy, or congenital defects, among other factors, are likely the most predisposed to severe health complications (Hall et al, 1986). In fact, for immunodeficient patients who develop pneumonia, death rates have been estimated as high as 80% (Englund et al, 1988; Welliver 2003).

Interestingly, RSV infection is frequently found in tandem with other types of infections, and has also been suggested as a risk factor for certain illnesses (Chappell et al, 2013; Thorburn et al, 2006). Perhaps most notably, RSV is often associated with increased respiratory tract bacterial loads, such as *Streptococcus pneumoniae* and *Staphylococcus aureus* (Chappell et al, 2013). For infants admitted to pediatric intensive care units (PICU) because of RSV-induced bronchiolitis, previous studies have found that the incidence of bacterial co-

infections is as high as 44% (Duttweiler et al, 2004; Randolph et al, 2004). Nonetheless, while several studies have reported these findings, it remains somewhat unclear whether there is a correlation between the degree of RSV severity and the presence of bacterial co-infections (Chappell et al, 2013). Numerous studies have also proposed an association between RSV infection and acute otitis media (middle ear infection) (Arola et al, 1990; Chonmaitree et al, 1990). While otitis media is most often referenced as a bacterial condition, RSV is present in up to 40% of these cases, and some have suggested that the presence of both bacterial and viral pathogens leads to worse outcomes (Chonmaitree, 1990). Finally, it has been widely debated whether RSV-induced bronchiolitis is a risk factor for developing asthma (Bacharier et al, 2012; Pullan and Hey, 1982; Sigurs et al, 1995; Sigurs et al, 2000). While some studies have proposed a direct connection between RSV infection and the onset of asthma, others suggest patients suffering from asthma have a predisposition for bronchial obstructive disease, thus making them more susceptible to severe RSV infections early on in life (Pullan and Hey, 1982; Sigurs et al, 1995; Sigurs et al, 2000).

### 1.4 Respiratory syncytial virus genome

RSV contains a negative-sense, 15.2 kilobase non-segmented RNA genome composed of 10 genes, which code for 11 proteins (see **Figure 1.2**) (Bawage et al, 2013; Gonzalez et al, 2012). Located ahead of each gene is a gene-start (GS) motif, which provides the signal for transcription initiation (Kuo et

al, 1996). Additionally, following each gene is a gene-end (GE) motif, which triggers transcription termination and transcript polyadenylation (Kuo et al, 1996). The precise mechanisms of RSV RNA transcription and replication are discussed in greater detail in **Section 1.5**. One can generally classify these genes into three main groups based on the function(s) of their protein products. There are three outer glycoproteins located on the viral surface: the small hydrophobic protein (SH), glycoprotein (G), and fusion protein (F) (Borchers et al, 2013). Generally, these outer proteins help form the viral coat, thus helping with RSV attachment and entry at the apical surface of airway epithelial cells (Bawage et al, 2013). While the role of the SH protein is not yet fully understood, studies suggest it may act as an immune-modulator through inhibition of tumor necrosis factor alpha (TNF-α) (Fuentes et al, 2007). The G protein is heavily glycosylated and helps to mediate cellular attachment, while the F protein (also a glycoprotein) promotes virus penetration, and formation of host cell syncytia [Ogra, 2004; Kuo et al, 1996). Recent studies suggest the F protein is necessary and sufficient for virus cell-entry, and this may be due to its interaction with a unique cellular receptor, possibly nucleolin (Mastrangelo and Hegele, 2013; Tayyari et al, 2011).

An additional five proteins are generally involved in RSV RNA replication and transcription (Borchers et al, 2013). These include the nucleoprotein (N), phosphoprotein (P), large polymerase (L), as well as two matrix proteins, named M2-1 and M2-2. Viral RNA associates with the helical nucleoprotein (N), forming the nucleocapsid complex (Tewar et al, 2009). The major polymerase subunit of

RSV is the L protein, which along with the P protein, associates with the nucleocapsid to help efficiently transcribe and replicate viral RNA (Borchers et al, 2013; Tewar et al, 2009). The M2-1 and M2-2 matrix proteins (produced from two overlapping reading frames of M2 mRNA) function as regulatory co-factors for this complex. While the M2-1 protein is an anti-termination factor promoting transcription, the M2-2 protein is thought to function as a regulatory "switch" from transcription to RNA replication (Bermingham and Collins, 1999). The nucleocapsid complex, in association with the L and P proteins, as well as the M2-1 and M2-2 cofactors, is generally referred to as the RSV RNA-dependent RNA polymerase complex (RdRp) (Mason et al, 2004; Tewar et al, 2009).

The last group of RSV proteins includes the matrix protein (M), along with two non-structural proteins, NS1 and NS2 (Borchers et al, 2013). The M protein is targeted to the nucleus early in the RSV life cycle, and later plays a critical role in virus assembly and budding of progeny RSV virions (Ghildyal et al, 2002; Ghildyal et al, 2003). Finally, the two nonstructural proteins of RSV, NS1 and NS2, function to evade the host immune response directed against RSV (Spann et al, 2004; Span et al, 2005).

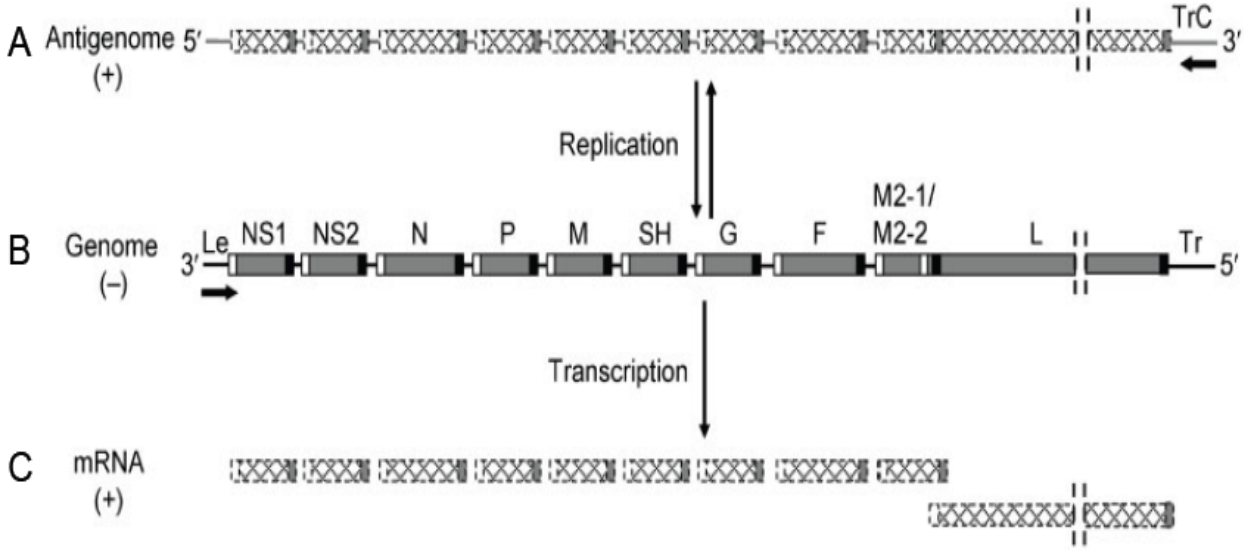


**Figure 1.2 The RSV genome**
The above figure represents the 15.2 kilobase non-segmented negative-sense single-stranded RNA genome of RSV **(B)**, along with the products of replication **(A)** and transcription **(C)**. Gene start (GS) and gene end (GE) sequences are represented by white and black boxes, respectively. Each of the RSV genes are depicted by grey boxes, and arrows represent the location of promoters. This figure has been adapted from Cowton et al, 2006.

## 1.5 Respiratory syncytial virus life cycle

While many aspects of the RSV life cycle have been clearly defined, there remain some significant gaps in knowledge. Preliminary attachment to the surface of airway epithelial cells is largely mediated by the G glycoprotein (Feldman et al, 1999; Feldman et al, 2000). This electrostatic interaction is controlled by a cluster of positively charged amino acids, known generally as the G protein's heparin binding domain (HBD), in both RSV subtype A ($^{184}$A➔T$^{198}$), and subtype B ($^{183}$A➔T$^{197}$) (Feldman et al, 1999; Feldman et al, 2000). These positively charged residues subsequently interact with negatively charged amino

acids located on highly sulfated heparin-like glycosaminoglycans (GAGs) on the cell surface (Feldman et al, 1999; Feldman et al, 2000). Fusion and subsequent penetration of the virus through the target cell membrane is initiated when the F protein binds its receptor (Feldman et al, 1999; Feldman et al, 2000). Previous studies indicate that the F protein is necessary and sufficient for virus cell entry, as deletions to both the outer G and SH glycoproteins have still resulted in RSV mutants (RSV ΔG ΔSH) capable of replicating both *in vitro* and *in vivo* (Crowe et al, 1996; Karron et al, 1997). The F protein is initially synthesized as an innactive 69 kDa precursor, $F_0$, which is cleaved by an intracellular furin-like protease at two amino acids, producing physiologically active disulphide-linked $F_1$ (49 kDa) and $F_2$ (20 kDa) proteins, which are then transported to the cell surface (Collins and Mottet, 1991; Gonzalez-Reyes et al, 2001). The identity of the cellular receptor(s) for the F protein, which presumably function to promote RSV penetration through the host cell membrane, has been widely debated for many years. Although some studies have shown that the F protein is also able to bind extracellular heparin-like GAGs, more recently it was claimed that nucleolin was the main receptor (Feldman et al, 2000; Mastrangelo and Hegele, 2013; Tayyari et al, 2011). Nucleolin is a multifunctional and ubiquitous protein located both within, and on the surface of eukaryotic cells, and is already known to be the extracellular receptor for other molecules such as laminin-1 and apoB/E-containing lipoproteins, among others (Mastrangelo and Hegele, 2013). However, it remains very plausible that the F protein may interact with multiple extracellular

receptor and co-receptor molecules (Tayyari et al, 2011). This is supported by the fact that RSV has a restricted tropism to the respiratory tract, yet nucleolin is a protein found in all cells (Collins et al, 2013). While the F protein is necessary to promote entry into the cell, the exact mechanism by which it does this is still up for debate. While some have suggested direct fusion and entry, there is also evidence for clathrin-mediated endocytosis (Collins et al, 2013; Cowton et al, 2006; Kolokolsov et al, 2007; Mastrangelo and Hegele, 2013). Despite this mechanistic debate, there is a consensual agreement that this process is pH-independent (Collins et al, 2013).

Fusion and entry into host cells triggers release of the RdRp complex, along with other internal proteins from the viral particle (Cowton et al, 2006). Cytoplasmic inclusion bodies (IBs) composed primarily of the L polymerase and associated transcription and replication proteins can be detected as early as 12 hours post-infection (Collins et al, 2013; Cowton et al, 2006). These IBs are generally regarded as RNA synthesis “factories” (Cowton et al, 2006). At this point, P protein, acting as a transcriptional cofactor, guides the L polymerase to the RNA-N nucleocapsid complex (Collins et al, 2013). L protein initiates the transcriptional process at the promoter region located at the 3’ leader (Le) sequence (see **Figure 1.3A**) and transcribes viral RNA towards the 5’ trailer (Tr) sequence in a start-stop fashion (Collins et al, 2013). At each GE signal, polyadenylation of the mRNA fragment is triggered, and the polymerase also receives a concurrent signal making it responsive to the next GS region (Kuo et

al, 1996; Fearns and Collins, 1999). While the N, P, and L proteins are the minimum components required for transcription, efficient transcription is largely dependent on the presence of the M2-1 transcriptional cofactor (Collins et al, 2013). Despite the anti-termination activity of the M2-1 protein, there remains a slight tendency for the polymerase to dissociate in between gene segments, thus genes at the 5' end are typically transcribed to a slightly lesser degree (Cowton et al, 2006). Interestingly, the M2-1 and M2-2 reading frames overlap slightly in the RSV genome (Collins et al, 2013; Fearns and Collins, 1999). It has been demonstrated that the polymerase is able to backtrack during transcription in a process known as retrograde scanning (Fearns and Collins, 1999). The random overlap in gene sequences is thought to confer no disadvantage to the virus because of the intrinsic backtracking capabilities of the polymerase (Collins et al, 2013).

Following transcription, translation of RSV genes occurs using the host cell machinery (Collins et al, 2013). The molecular switch from transcription to RNA replication is thought to occur when a threshold level of N protein is produced that will allow encapsulation of newly synthesized viral RNA (Bermingham and Collins, 1999). In contrast to transcription, the L polymerase reads through the entire genome, producing a full-length antigenome, which is then replicated prior to association with newly synthesized N proteins (Collins et al, 2013). The exact signal(s) directing the switch to replication are not fully known, however there has been some progress in delineating this process. Firstly, the first 34 nucleotides at

the 3' end of the genome (upstream of the first GS signal) are needed to produce full-length encapsulated RNA (Cowton and Fearns, 2005; McGivern et al, 2005). Secondly, the M2-2 protein appears to also play an essential role (Bermingham and Collins, 1999). Mutant RSV strains lacking the M2-2 gene (ΔM2-2) fail to switch from transcription to replication, thus implicating the M2-2 protein as a key component in this process (Bermingham and Collins, 1999).

During both the transcription and replication processes, several other RSV proteins concurrently play key roles in the viral life cycle. As previously stated, the exact role of the SH protein is still largely unknown. While reported to be a possible viroporin, modifying membrane permeability, the SH protein may also help promote RSV survival by inhibiting antiviral cytokines, such as TNF-α (Fuentes et al, 2007). Early in infection, the M protein is localized to the nucleus where it is thought to play a role in inhibiting host-cell transcription (Ghildyal et al, 2003). The M protein has also been shown to enhance RSV pathogenesis by inducing epithelial cell cycle arrest via a p53-dependent pathway (Bian et al, 2012). Furthermore, the two non-structural proteins, NS1 and NS2, are both involved in interfering with innate immune responses directed towards RSV infection (Bitko et al, 2007). For example, both proteins have been shown to impair interferon signaling, and also impair cellular apoptosis (Bitko et al, 2007; Spann et al, 2005). Their important roles in defending against the immune system help explain why they are the most abundantly produced proteins in the RSV genome (Collins et al, 2013).

Following both transcription and RNA replication, RSV proteins are targeted to the apical surface of the cellular membrane in preparation for virus budding. The release of progeny virions peaks at approximately 24 hours post-infection (Collins et al, 2013). The RSV budding process is intricate and not fully understood, as components of the RdRp complex and the outer glycoproteins are separately targeted to the same membrane region. These areas are described as lipid-raft structures with certain calveolae-like properties (Brown et al, 2004). The F protein is targeted to the cell membrane with its transmembrane domain through the secretory pathway, and is also thought to play a key role in targeting other viral components to this region (Batonick and Wertz, 2011). For example, deletion of the F protein was previously shown to result in decreased levels of G and SH proteins being incorporated into progeny virions (Batonick and Wertz, 2011). Lower levels of the G and SH proteins also result in decreased levels of RdRp proteins being targeted to the membrane (Batonick and Wertz, 2011). This assembly feature of the F protein is controlled through its cytoplasmic tail, as viral filaments fail to form in mutant RSV strains lacking this domain (Baviskar et al, 2013). Interestingly, while the M protein is targeted to the nucleus during early infection, it appears to also play an essential role in both RSV assembly and budding. Deletion of the M protein results in poor localization of RdRp proteins to the cell membrane, thus hinting that the M protein is involved in targeting these complexes from cytoplasmic IBs to budding sites (Mitra et al, 2012). It has previously been suggested that localization of M with these proteins also silences

RSV RNA synthesis, which is further supported by the fact that M proteins are sequestered in the nucleus during early infection (Ghildyal et al, 2006).

Upon successful localization of all these components to lipid rafts, the exact mechanism of RSV budding remains somewhat elusive (Utley et al, 2008). However, recent work has provided evidence that this process is primarily guided by both the F and M proteins (Baviskar et al, 2013). In this model, the F protein acts a catalyst, initiating the budding process by releasing previously assembled RSV protein complexes from its cytoplasmic tail, which are then to be incorporated into filamentous protrusions (Baviskar et al, 2013). M proteins form a layer under the plasma membrane, and interact with F proteins just prior to budding (Baviskar et al, 2013). Morphological changes induced by these M proteins are critical for elongation of filamentous protrusions and virus budding (Baviskar et al, 2013; Mitra et al, 2012). For example, it was recently demonstrated that M proteins must oligomerize into dimers to help RSV virions elongate and bud off the membrane (Forster et al, 2015). Mutations at this dimerization interface prevent the formation of filaments; as such this process is thought to be an essential final step in RSV virion production (Forster et al, 2015). A general schematic representing the complete RSV life cycle, including all the essential viral proteins, is depicted below in **Figure 1.3**.

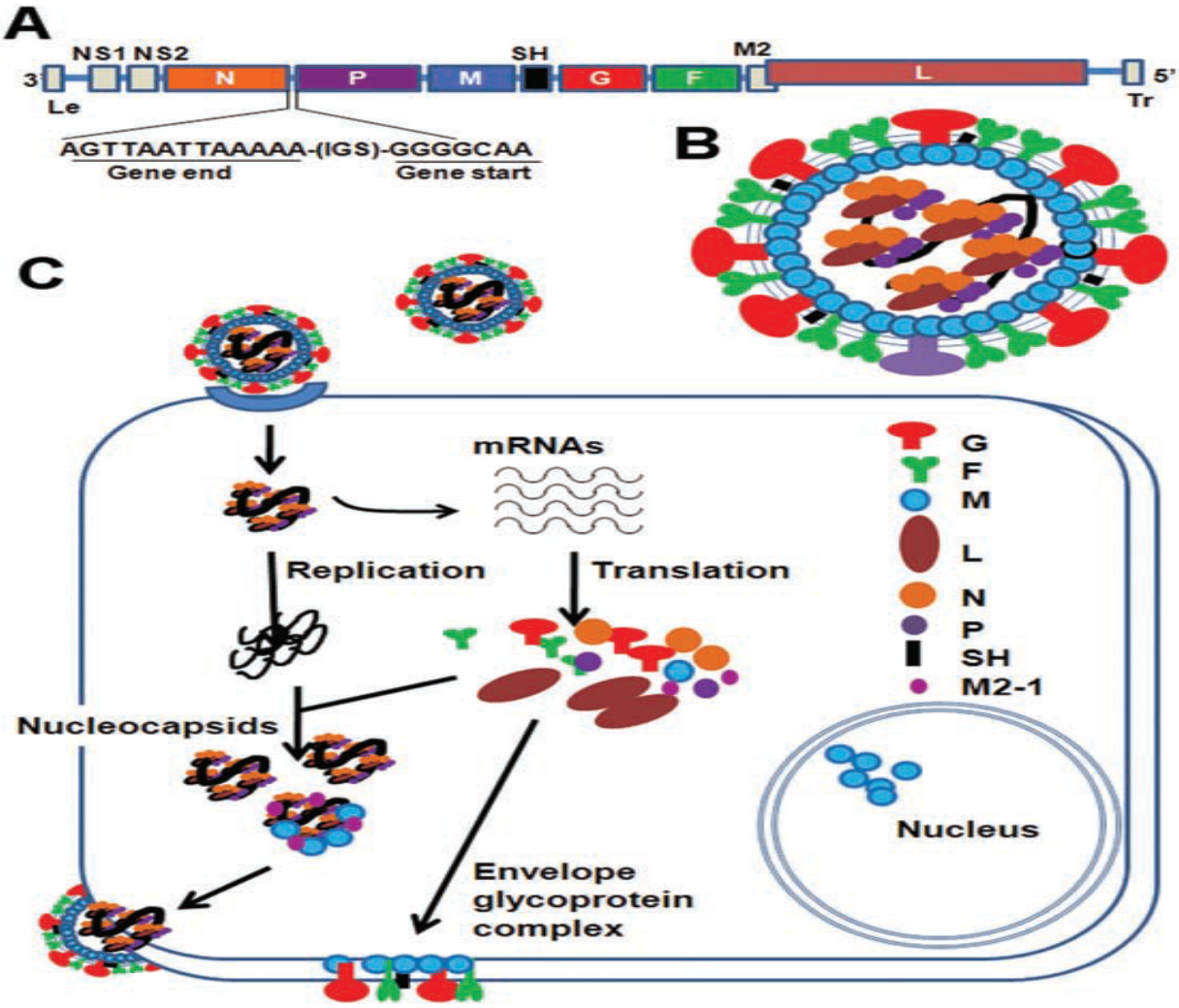


**Figure 1.3 Generalized RSV life cycle.**
**(A)** The RSV genome is 15.2 kilobases in length, and includes 10 genes that code for 11 proteins. **(B)** General schematic of the RSV virion structure. The negative-sense RNA genome is found in association with the RdRp complex, and is encapsulated by a glycoprotein coat. **(C)** RSV life cycle in infected cells. RSV attachment is mediated through the G protein, which binds to extracellular GAGs by electrostatic interactions. Viral entry is triggered by F, possibly through binding to a nucleolin receptor. The virus is then internalized (mechanism unknown) and its inner contents are released into the cytoplasm. During the early stages of infection, the M protein is localized to the nucleus. The RdRp complex first transcribes viral RNA into 11 individual monocistronic mRNAs, which are then translated by host cell machinery. A threshold level of N protein triggers a molecular "switch" to viral RNA replication (aided by the M2-2 protein), thus producing a full-length positive sense antigenome. The antigenome is then replicated into its negative-sense counterpart for packaging into progeny virions. Surface glycoproteins are translated in the ER, glycosylated in the Golgi apparatus, and localized to the cell membrane at lipid rafts. The M protein localizes with the RdRp complex late in infection, thus also helping to target these proteins to lipid rafts. Finally, progeny virions are released from the host cell as filamentous protrusions. This figure is taken from Ghildyal et al 2010.

## 1.6 Phosphoprotein overview

The RSV P protein has a predicted molecular weight of 27 kDa, and is composed of 241 amino acids (Llorente et al, 2006). However, it should be noted that when run alone on SDS-PAGE gels, it typically displays a greater molecular weight in the range of 33 kDa to 35 kDa (Bangham et al, 1986; Castagne et al, 2004). Previous research showed that deletions spanning amino acids 200-220 of P completely altered its apparent molecular weight on SDS-PAGE gels, which suggests this domain may be responsible for the abnormal gel migration pattern (Tran et al, 2007). In comparison to P proteins from other members of the paramyxovirus family, the RSV P protein is much smaller (Lu et al, 2002). As will be later described in **Section 1.8**, the P protein represents an intriguing target for RSV therapeutics, and is one of the main focuses of this thesis. P proteins are a necessary component of the RSV RdRp complex, and are known to interact with itself, the N protein, L protein, and the M2-1 cofactor (Galloux et al, 2012). Similar to relatives such as the Sendai virus, the RSV P protein has been shown to form homotetrameric complexes, with an α-helical oligomerization domain mapped between centrally-located residues 120 to 150 (Ajenso and Villanueva, 2000; Castagne et al, 2004; Llorente et al, 2006).

Within the virus core, as well as within infected cells, P protein remains constitutively phosphorylated (Lu et al, 2012). The bulk of P protein phosphorylation in mediated by casein kinase II on centrally located serines 116, 117, and 119, as well as serines 232 and 237 in the C-terminal region (Fuentes

et al, 2000; Lu et al, 2012; Mazumder and Barik, 1994; Villanueva et al, 2000). Other less prominent sites of phosphorylation have also been suggested at additional serine and threonine residues (Ajenso et al, 2006; Navarro et al, 1991). Over the years, there has been much debate on the exact role and necessity, if any, of RSV P protein phosphorylation. While it was initially suggested that phosphorylation of the P protein is necessary to carry out RSV transcription *in vivo*, it was later demonstrated that impaired phosphorylation in Hep-2 cells did not abrogate transcription or RNA replication (Barik et al, 1995; Villanueva et al, 1991). Later research using an RSV minigenome assay reported that while phosphorylation of P protein is not necessary to carry out virus replication, it is required for efficient replication both *in vitro* and *in vivo* (Lu et al, 2002). The molecular switch between RSV transcription and replication may also be guided through the aid of P protein phosphorylation and dephosphorylation cycles. Phosphorylation of threonine 108 has been shown to prevent binding between P and M2-1, which subsequently would affect the ability of M2-1 protein to interact with the L polymerase and influence the transcription process (Ajenso et al, 2006).

The precise intracellular function of the P protein in RSV pathogenesis is fairly well characterized, as are its binding domains with other RSV proteins. The P protein is thought to function as an essential cofactor by helping to position the L polymerase on the helical nucleocapsid, thereby contributing to the initiation and maintainance of RNA transcription and replication (Esperante et al, 2012;

Tran et al, 2007). This is a mechanism common to many members of the paramyxovirus family (Esperante et al, 2012). Through the use of recombinant proteins containing specific mutations, the L protein binding site on the P protein was recently mapped to amino acids 212 to 239 of the C-terminal domain (Sourimant et al, 2015). When bringing the L polymerase into contact with the N-RNA nucleocapsid complex, the P protein also makes essential contact with N protein (Murray et al, 2001; Tran et al, 2007). This N-P protein association is one of the most well characterized protein-protein interactions involved in RSV pathogenesis. Mutant N and P glutathione S-transferase (GST) fusion proteins (ΔN, ΔP) have been used in pull-down studies to map their binding domain (Tran et al, 2007). Initial research suggested that the C-terminus of the P protein interacted with the C-terminal arm of the N protein (Murray et al, 2001). A more recent study has demonstrated that the last 9 C-terminal acids of the P protein are both necessary and sufficient for binding to the N protein (Tran et al, 2007). Other findings using monoclonal antibodies specific to the C-terminus of the P protein suggest that an additional 12 C-terminal amino acids on the P protein may contribute to this interaction (Garcia-Barreno et al, 1996). Interestingly, the P protein is also thought to function as a molecular chaperone for newly synthesized N protein, referred to as $N^{\circ}$, which helps to maintain it in a soluble state (Esperante et al, 2012; Galloux et al, 2015). This role is supported by the fact the crystal structure of the RSV N protein could only be determined when N protein was purified in complex with the P protein (Tawar et al, 2009). New light

has been shed on this N°-P association through the use of a mutant form of monomeric N protein that is unable to bind viral RNA (Galloux et al, 2015). This work demonstrated that N-terminal amino acids 1 through 29 of P are sufficient for binding to N° (Galloux et al, 2015; Karlin and Belshaw, 2012). Thus, it appears that while the C-terminus of the P protein is essential for binding N protein in complex with RNA, the chaperone function of the P protein is likely controlled through its N-terminal domain (Galloux et al, 2015). Taken together, the N-P protein interaction in RSV represents an intriguing target for therapeutic discovery, which will be discussed further in **Section 1.8**.

RSV P protein binding with other intracellular viral and non-viral proteins has also been well documented. A centrally-located region in M2-1 ($M2\text{-}1_{58\text{-}177}$) was previously shown to interact with the N-terminus of the P protein in a 1:1 stoichiometry (Blondot et al, 2012; Esperante et al, 2012). While the exact mechanism(s) in which M2-1 protein is thought to prevent transcription termination has yet to be clarified, its interaction with P proteins is thought to play an essential role (Blondot et al, 2012; Esperante et al, 2012). Lastly, the P protein has been shown to bind to other intracellular non-RSV proteins, such as Heat-shock protein 70 (Hsp70). The function of this interaction is also somewhat unknown, although it has been suggested that Hsp70 may help maintain the N-P interaction, thus helping the L polymerase to efficiently transcribe and replicate viral RNA (Oliveira et al, 2013).

## 1.7 Current treatments

Over the years, there has been relatively little success in the world of RSV therapeutics. There is currently no vaccine to prevent RSV infection. Early excitement surrounding a formalin-inactivated (FI) RSV vaccine in the 1960's quickly turned to disappointment. As a result of this vaccine, several patients died, and greater than 80% of immunized children required hospitalization (Murphy and Walsh, 1988). While still not fully understood, follow-up research suggests epitopes of RSV surface glycoproteins were most likely modified by the formalin treatment, thus patient serum antibodies were significantly reduced in their ability to effectively neutralize viral particles (Murphy and Walsh, 1988). Autopsy results confirmed these poorly neutralizing antibodies resulted in the deposition of immune complexes in certain tissues (Polack et al, 2002). There was also a severe infiltration of both monocytes and neutrophils to the bronchiolar epithelium (Prince et al, 2001). Furthermore, it appears as though the FI RSV vaccine induced a strongly polarizing type 2 helper T cell (Th2) response (Jorquera et al, 2013). In addition to having elevated Th2 cytokines such as IL-4 and IL-13, patients also displayed clinical features characteristic of Th2 responses, including wheezing, mucus hypersecretion, and airway obstruction (Graham, 2011; Jorquera et al, 2013; Tang and Graham, 1994). The aforementioned cytokines have also previously been linked to poor virus-specific CD8+ cytotoxic T lymphocyte (CTL) function and ineffective viral clearance (Graham, 2011; Jorquera et al, 2013; Tang and Graham, 1994). While some

progress has been made in developing a viable vaccine candidate since this time, there remain significant hurdles. Firstly, because RSV commonly infects children at a young age, they have underdeveloped cellular and humoral immune responses (Borchers et al, 2013; Murata, 2009; Schickli et al, 2009). The presence of maternally-derived antibodies at birth can also lead to poor mucosal and serum antibody responses, possibly due to antigen sequestration (Borchers et al, 2013; Murata, 2009; Schickli et al, 2009). Additionally, any potentially useful RSV vaccine must avoid cross-reactions with the numerous other vaccines typically received during infancy, which could decrease their overall effectiveness (Borchers et al, 2013; Murata, 2009; Schickli et al, 2009). Finally, testing potential vaccines in humans is also an issue. Older subjects have typically already developed an immunologic memory to RSV and thus will respond differently than infants (Borchers et al, 2013; Murata, 2009; Schickli et al, 2009). There is some hesitancy in testing RSV vaccine candidates in young infants following the failure of the FI RSV vaccine (Rudraraju et al, 2013).

Current treatment for RSV infection is determined on a case-by-case basis, primarily due to the potential presence of other illnesses, for example, bacterial co-infections. Management of RSV-induced bronchiolitis or pneumonia is mainly supportive in nature, and often includes oxygen therapy, intravenous fluids, and bronchodilators (Borchers et al, 2013). Ribavirin is currently the only antiviral drug approved to treat RSV infection (Bawage et al, 2013; Borchers et al, 2013; Turner et al, 2014). The latter is a broad-spectrum antiviral drug, which has

several proposed direct and indirect mechanisms of action (Bawage et al, 2013; Borchers et al, 2013; Turner et al, 2014). As a guanosine analog, ribavirin can be directly incorporated into the RSV genome, interfering with polymerase activity and causing direct mutagenesis, thereby decreasing RSV replication efficiency (Bawage et al, 2013; Borchers et al, 2013; Turner et al, 2014). Indirectly, ribavirin competitively inhibits inosine monophosphate dehydrogenase (IMPDH), causing depletion of intracellular guanosine-5'-triphosphate (GTP) and mRNA guanylyl transferase (Bawage et al, 2013; Turner et al, 2014). Interestingly, ribavirin is also thought to have indirect immunomodulatory effects, such as upregulation of interferon-stimulated response element (Bawage et al, 2013; Beaucourt and Vignuzzi, 2014; Turner et al, 2014). Unfortunately, because of high costs, coupled with prolonged aerosol administration, as well as controversy regarding its overall effectiveness, use of ribavirin in clinical settings is still fairly limited (Barry et al, 1986; Borchers et al, 2013; Turner et al, 2014). Current research suggests ribavirin is most effective in treating young infants or immunocompromised lung transplant patients at risk of mortality from acute RSV infection (Turner et al, 2014).

Other than ribavirin, the only other Federal Drug Administration (FDA)-approved drug for RSV infection is palivizumab (also known as Synagis), a monoclonal antibody targeting the RSV F glycoprotein (Bawage et al, 2013; Borchers et al, 2013; Rodriguez and Ramilo, 2014). Palivizumab is currently used specifically for prophylaxis in high-risk infants, such as those with congenital

heart disease, chronic lung disease, or premature birth prior to 32 weeks (Bawage et al, 2013; Borchers et al, 2013; Rodriguez and Ramilo, 2014). Previous clinical trials have demonstrated that such prophylaxis decreases RSV hospitalization rates for prematurely born infants by 78%, and 39% for those with chronic lung disease (Impact-RSV Study Group, 1998). Motavizumab, a monoclonal antibody derived from affinity maturation of palivizumab, showed greater RSV-neutralization capabilities in early pre-clinical trials (Rodriguez and Ramilo, 2014). However, due to an increased rate of subcutaneous reactions, coupled with Palivizumab having an excellent safety record, Motavizumab was not FDA-approved (Rodriguez and Ramilo, 2014).

Several new avenues are currently being explored as novel treatments for RSV infection. Clinical trials are ongoing for antiviral agents and vaccine candidates. The most notable antivirals include the Gilead fusion inhibitor, GS-5806, and Alios'

ALS-008176 compound (Mejias and Ramilo, 2015; Murray et al, 2014). GS-5806, a small molecule inhibitor which targets the RSV F protein to block viral fusion to the host cell membrane, is currently in phase-II clinical trials (Mejias and Ramilo, 2015; Murray et al, 2014). ALS-008176 is a small molecule nucleoside analog which targets the RSV polymerase, and is currently in phase-I clinical trials (Mejias and Ramilo, 2015; Murray et al, 2014). Another interesting avenue in RSV antiviral research involves small interfering RNA (siRNA). ALN-RSV01, an RSV N protein-specific siRNA, was shown to have antiviral activity and preserve

lung function in lung transplant patients (Mejias and Ramilo, 2015; Murray et al, 2014). Not only are some of these antiviral compounds being researched for use in the high-risk infant population, but in adults as well (Mejias and Ramilo, 2015). Some new vaccines are also in their early stages of testing, however there has been a relative lack of success in developing viable candidates. While many of these potential vaccines have shown protective abilities in mice or cotton rats, this success has not translated well to clinical trials (Borchers et al, 2013). The most traditional approach in developing RSV vaccines has been to produce live attenuated temperature-sensitive or cold-passaged mutants (Borchers et al, 2013; Murata et al, 2009; Schickli et al, 2009). Two notable candidates in this field are ΔNS2 Δ1313 I1314L and ΔM2-2, which are both currently in clinical trials (Murray et al, 2014). There is also a considerable amount of research focused on developing adjuvants capable of preventing Th2-response skewing and enhancing the overall immunogenicity of candidate vaccine preparations (Kamphuis et al, 2012; Zeng et al, 2012).

### 1.8 N-P interaction: plausible drug target

As was previously described, the RSV RdRp complex is absolutely necessary for full virulence. The main components of this complex are the N, P, and L proteins, as well as the M2-1 and M2-2 cofactors (Yu et al, 1995; Liuzzi et al, 2005). Among these various components, the N-P interaction is arguably the most well-characterized, and deletion of either of these proteins leads to a loss of

RSV replication and transcription abilities (Yu et al, 1995). While many RSV therapeutics have focused on targeting the outer surface-exposed glycoproteins, relatively less work has focused on intracellular targets. Compared to the outer glycoproteins, there is also less variability in the amino acid sequences of N and P between RSV subtype A and B, as well between different strains (Sullender et al, 2000). Taken together, this information suggests the RSV N-P interaction could be a novel, and potentially useful target for a putative RSV therapeutic. Disrupting this essential protein-protein interaction will the main focus of this thesis, as will be described in **Section 1.10**.

## 1.9 Peptide mimetic therapeutics

Peptide mimetics are small dominant negative molecules used to mimic and disrupt essential protein-protein interactions (Giuliani and Rinaldi, 2011; Olsen et al, 1993; Stone et al, 2011). Such interactions may be involved, for example, in biochemical molecular processes or intracellular signaling cascades. Generally, peptides are described as small proteins with 50 amino acids or less (McGregor, 2008). Since peptide mimetics are designed to bind a specific protein of interest, they can effectively be used to outcompete their full-length wild-type protein counterpart. While peptides present themselves as useful therapeutics due to their specificity towards their targets and small size, there are several barriers that can hamper their overall effectiveness. For example, if their target is located within cells, there needs to be a built-in mechanism targeting the peptide

to this region, and secondly, peptides are often rapidly degraded in the presence of host proteases (Giuliani and Rinaldi, 2011; Mason, 2010; Olsen et al, 1993; Stone et al, 2011). In order to help avoid proteolytic degradation, peptide mimetics can be designed such that the peptide is conjugated to a carrier molecule, thereby increasing their overall half-life (Werle and Bernkop-Schurch, 2005). Furthermore, intracellular targeting of peptide mimetics can be achieved through conjugation to a cell-penetrating peptide (CPP) sequence (Mason, 2010).

Numerous other studies have previously employed peptide mimetics in their research with considerable success (Ahren and Schmitz, 2004; Kwong et al, 2011; Sonne et al, 2008). For example, a peptide that mimics human CD4 and CCR5 receptors, thus targeting the HIV-1 gp120 glycoprotein, effectively prevented entry of HIV-1 into cells expressing these receptors (Kwong et al, 2011). Other peptide mimetic therapeutics have already been approved for clinical use by the FDA. Glucagon-like peptide 1, also known as Byetta or Exenatide, is a peptide mimetic approved for treatment of diabetes mellitus type 2, and functions by increasing glucose-dependent insulin secretion (Ahren and Schmitz, 2004; Sonne et al, 2008). The Mahony laboratory has previously used peptide mimetics to target intracellular protein-protein interactions in both bacterial and viral (unpublished) pathogens (Stone et al, 2011). These studies involved targeting both the *Chlamydia pneumonia* Type III Secretion System (T3SS), and the Influenza Polymerase Basic Protein 1 (PB1) (Stone et al, 2011).

1.10 Thesis objectives: targeting RSV using a phosphoprotein mimetic

Taking from success in using peptide mimetics to target pathogens such as *Chlamydia pneumonia* and Influenza, coupled with the fact that several peptide mimetic therapeutics have been FDA-approved, this therapeutic model presented itself as a unique candidate for targeting other viruses like RSV. The purpose of this Master's thesis was to extend the success achieved with these mimetics towards RSV. Based on previously published research mentioned in **Section 1.9**, which outlined the necessity of N-P binding for RSV pathogenesis, this interaction presented itself as an ideal candidate for a novel chimeric peptide mimetic inhibitor. It was thus hypothesized that a peptide mimetic containing the C-terminal N protein binding domain of the RSV P protein would prevent binding of the full-length P protein to the N protein, thereby disrupting assembly of the core polymerase complex, and inhibit RSV propagation *in vitro*. In this thesis, we cloned and successfully purified this phosphoprotein mimetic, named $P_{220\text{-}241}$, which contained the final 21 C-terminal amino acids of the RSV P protein linked to a CPP, *E. coli* Maltose-Binding Protein (MBP), and a polyhistidine tag; thus forming a novel HisMBP-CPP-$P_{220\text{-}241}$ chimeric construct of approximately 47 kDa (see **Supplementary Figure S1**). Please note that for simplicity this construct will simply be referred to as $P_{220\text{-}241}$ for the remainder of this thesis.

Using *in vitro* RSV inhibition assays, we showed that purified $P_{220\text{-}241}$ is able to successfully enter cells and subsequently inhibit both replication and release of progeny RSV virions. Using a series of toxicity assays, we

demonstrated that $P_{220-241}$ did not have any cytotoxic effects towards multiple cell lines. It was also shown that viral inhibition was not a secondary effect caused by the mimetic acting as a pathogen-associated molecular pattern (PAMP). The mechanism of the mimetic was then investigated. We were able to show using both GST pull-down assays and a series of *in vitro* co-immunoprecipitations experiments that $P_{220-241}$ was able to bind RSV N protein and prevent binding of full-length P protein, as was originally hypothesized.

# CHAPTER TWO

# MATERIALS AND METHODS

## 2.1 Construction of expression plasmids

For the RSV $P_{220-241}$ construct, an overlapping Polymerase Chain Reaction (PCR) was employed as previously described to create chimeric amplicons containing the nucleotide sequence for the CPP sequence (YGRKKRRQRRR), and the final 21 C-terminal amino acids of RSV P protein (EKLNNLLEGNDSDNDLSLEDF) (Heckman and Pease, 2007). The PCR primers contained *attB* recombination sites in order to allow compatibility with the Gateway® Cloning System. Presence of amplicons of the correct size was confirmed by DNA gel electrophoresis on a 0.6% agarose gel (see **Section 2.5.1**). The purified amplicon was cloned into the $pDONR_{201}$ vector via the Gateway® BP reaction to produce the pENT vector. For all other expression plasmids, gBlock gene fragments (Integrated DNA Technologies, Coralville IA) were designed to contain nucleotide sequences of the desired protein product, flanked by *attB* recombination sites. These gene fragments were then added to the Gateway® BP reaction, according to the manufacturers protocol. To do this, Gateway® BP clonase was incubated with both the $pDONR_{201}$vector and either the purified $P_{220-241}$ DNA, or the gBlock gene fragments, for 1 hour in the presence of TE buffer (1 mM EDTA and 10 mM Tris pH 8.0). The BP reaction was terminated with the addition of 0.2 µg/µL Proteinase K (Invitrogen) for 10 minutes at 37°C. The resultant pENT vector was transformed into chemically competent *E. coli* Turbo cells (New England Biolabs, Ipswich MA) and plated on

Luria Bertani (LB) (1% w/v tryptone, 0.5% w/v yeast extract, 1% w/v NaCl) plates containing 100 µg/mL of ampicillin. The plasmid was purified from successful transformants to be used in a Gateway® LR reaction. Gateway® LR clonase was incubated with both the pENT vector and the desired pDEST vector (e.g. pDEST HisMBP) for 1 hour in the presence of TE (Tris-EDTA) buffer. Proteinase K (0.2 µg/µL) was once again used to terminate the reaction. The expression plasmids were subsequently transformed into either chemically competent *E. coli* BL21 (DE3) cells or Rosetta (DE3) (for enhanced expression of rare codons), which were stored at -80°C in 15% sterile glycerol. All constructs were verified by sequencing from MOBIX laboratory at McMaster University.

### 2.2 Chemically competent *E. coli* cell preparation

*E. coli* BL21 (DE3), Rosetta (DE3) (Life Technologies, Burlington ON), or Turbo cells were grown overnight in LB broth while shaking at 37°C. These cells were then re-inoculated into fresh LB broth at a dilution of 1:100, and allowed to grow under the same conditions. Once the cells reached an optical density at 600 nm ($OD_{600}$) of approximately 0.5, they were cooled on ice for 15 minutes, and then centrifuged for 10 minutes at 3000 RPM and 4°C. The cells were resuspended in ice cold 10mM $MgSO_4$, allowed to incubate on ice for 30 minutes, and then centrifuged as previously described. Harvested cells were then resuspended in ice cold 50 mM $CaCl_2$, allowed to incubate on ice for an additional 30 minutes, and centrifuged for a final time as previously described.

The cells were then resuspended in 50 mM $CaCl_2$ containing 15% (v/v) sterile glycerol before being aliquoted and stored at -80°C for future use.

### 2.2.1 *E. coli* transformation

Chemically competent *E. coli* cells were thawed on ice and approximately 150 ng purified DNA (in sterile distilled $H_2O$) was added to incubate for 30 minutes. The cells were then subjected to heat shock at 42°C for 45 seconds, incubated on ice for 2 minutes, and resuspended in 700 µL of SOC media (2% w/v tryptone, 0.05% w/v NaCl, 0.5% w/v yeast extract, 4 mM glucose, 10 mM $MgCl_2$). Following a 1 hour incubation at 37°C, the cells were plated on LB plates containing 1.5% (w/v) agar and either 100 µg/mL ampicillin or 30 µg/mL kanamycin. The plates were allowed to incubate overnight at 37°C before selecting individual bacterial colonies.

### 2.2.2 Recombinant protein expression and FPLC purification

All constructs were expressed in either *E. coli* BL21 cells (DE3) or Rosetta (DE3) cells. LB broth (6 L) containing 100 µg/mL of ampicillin was inoculated with 100 mL of overnight culture, and incubated at 37°C and 250 RPM until the cultures reached an optical density $OD_{600}$ of approximately 0.6. Expression of recombinant proteins was then induced with the addition of 0.5 mM isopropyl β-D-thiogalactopyranoside (IPTG). The exact time, and temperature for protein expression (at 250 RPM) was optimized for each of the expression plasmids. The

cells were harvested at 8000 x g for 4 minutes at 4°C. Cells used to express polyhistidine-tagged proteins were resuspended in 15 mL of ice cold Nickel A buffer (20 mM Tris-HCl pH 7.0, 0.03% LDAO, 0.02% β-mercaptoethanol, 500 mM KCl, 10% glycerol, 10 mM imidazole) with one EDTA-free protease inhibitor tablet (Roche, Laval QC), while cells used to express GST-tagged proteins were resuspended in ice cold sterile 1X phosphate buffered saline (PBS). At this point, GST-tagged recombinant protein lysates were stored at -80°C. For polyhistidine-tagged proteins, the cells were subsequently lysed (on ice) via sonication with the Fischer Scientific Sonic Dismembrator (Model 100) 6 times at 25 watts (W) for 20 seconds. Soluble protein was separated from the insoluble pellet of lysed cells by centrifugation at 42,000 x g for 45 minutes at 4°C. The supernatant was vacuum filtered through a 0.22 μM bottle filter (Fisher Scientific, Whitby ON) and stored on ice prior to purification.

Recombinant polyhistidine-tagged proteins were purified with Fast Protein Liquid Chromatography (FPLC) using the AKTA FPLC (GE Healthcare, Mississauga ON). The filtered lysates were run through a His-Trap™ column charged with 100 mM of $NiCl_2$. The proteins were eluted in Nickel B buffer (same contents as Nickel A, except it contains 300 mM of imidazole) and stored on ice before being buffer exchanged into 1X sterile PBS using the HiPrep 26/10 Desalting Column (GE Healthcare, Mississauga ON). Purified protein solutions were vacuum filtered through a 0.22 μM filter and concentrated at 3000 RPM and 4°C using an Amicon Ultra-15 Centrifuge Filter (Millipore, Billerica MA). Proteins

were stored at 4°C for immediate use, or -80°C for future experiments.

### 2.2.3 Quantifying protein concentration

To assess the presence and overall purity of the recombinant proteins, a fraction of the final protein sample was collected and resuspended in 2X Laemmli buffer (4% (v/v) SDS, 100 mM Tris pH 7.0, 2 mM EDTA, 10% (v/v) glycerol, 0.002% (w/v) bromophenol blue, 10% (v/v) β-mercaptoethanol) before being electrophoresed on a 12% SDS-PAGE gel. The gel was then treated with Coomassie stain to visualize protein purity. To evaluate protein concentration, a modified version of the Lowry assay was used (Lowry et al, 1951). A small aliquot of purified protein was incubated with 127.5 µL of Reagent A (containing copper sulfate) followed by 1 mL of reagent B (dilute Folin reagent) according to the manufacturers protocol (Bio-Rad, Mississauga ON). This assay was then repeated with varying concentrations of Bovine Serum Albumin (BSA) in 1X PBS. Absorbance measurements were taken at 750 nm and protein concentration was determined in reference to a BSA standard curve.

## 2.3 Cell culture

LLC-MK2 (Rhesus monkey kidney cells) and BEAS-2B (human lung bronchiolar epithelial cells) (ATCC, Manassas VA) were used in this study. Both of these cell lines were grown in Dulbecco's Modified Eagle Medium (DMEM)

(Invitrogen, Mississauga ON) supplemented with 10% heat-inactivated fetal bovine serum (FBS) (Invitrogen) at 37°C and 5% $CO_2$. Every 2 to 10 days, the cell medium was removed, and the monolayer was washed with 1 mL of Trypsin-EDTA (Invitrogen). The cells were then treated with an additional 5 mL of Trypsin-EDTA for 5 minutes at 37°C and 5% $CO_2$. Depending on the experiment, the trypsinized cells were then resuspended in fresh DMEM+10% FBS and added to an appropriate culture flask (i.e. T25, T75, or T175).

To count cells prior to seeding, trypsinized cells were centrifuged at 500 x g for 5 minutes and resuspended in 5 mL of DMEM+10% FBS. An aliquot of 10 µL containing a 1:1 dilution of cells and Trypan blue reagent was plated on a Bright-Line Hemacytometer (Hausser Scientific, Horsham PA). The number of cells per mL was determined by averaging the number of viable cells within each of the quadrants of the hemacytometer. The number of cells per mL of medium was calculated using the following equation: #cells/mL=[average number of cells per quadrant x 2 (dilution factor) x 10,000 cells/mL]

### 2.4 Virus culturing

The following virus strains (stock cultures at unknown titers) were obtained from the St. Joseph's Hospital virology laboratory: RSV A Long strain, RSV B CH-18537 strain, and PIV-2. To propagate each of the virus isolates, 1 mL aliquots of frozen stocks were thawed and added to 9 mL of R-Mix Refeed Medium (Diagnostic Hybrids, Athens OH). The virus and cell medium solutions

were then added to a confluent monolayer of LLC-MK2 cells in a T75 flask. The flasks were incubated at 37°C and 5% $CO_2$ for 7 to 8 days for RSV strains and 4 to 5 days for PIV-2. Cell monolayers were monitored on a daily basis for cytopathic effects by comparing infected cells to those in a control T75 flask containing no virus. To harvest virus, the monolayers were scraped off using a cell scraper or the end of a sterile pipette. The infected cell and medium solution was then transferred to a falcon tube and vortexed with sterile glass beads 2 times for 30 seconds. The solution was then decanted and subsequently passed through a 0.22 µM filter. Aliquots ranging from 100 µL- 1 mL were stored at -80°C for future use.

To determine an ideal virus concentration to use in inhibition experiments (see **Sections 2.7.1 and 2.7.2**), serial dilutions of frozen virus stocks were made in DMEM, with final volumes of 400 µL. These solutions were added to shell vials containing confluent LLC-MK2 cell monolayers, and were centrifuged for 30 minutes at 1,500 x g (centrifugation-assisted inoculation), followed by a 30 minute incubation period at 37°C and 5% $CO_2$. The viral medium was then removed, and the cells were treated with DMEM alone. The cells were allowed to incubate for 48 hours at 37°C and 5% $CO_2$ for those treated with RSV, and 24 hours for those treated with PIV-2. After these time periods, the medium was removed, and the cells were fixed with 1 mL of ice-cold acetone for 30 minutes at room temperature. After aspirating the acetone, the cells were washed twice with sterile 1X PBS and treated in the dark with D-Ultra Respiratory Virus Screening

DFA Reagent (Diagostic Hybrids) for 30 minutes at 37°C and 5% $CO_2$. After being washed three times with sterile 1X PBS, the cover slips were mounted face down on glass slides with 10 µL of mounting media (50% glycerol and sterile 1X PBS). The cover slips were visualized with fluorescent microscopy at 10X magnification using the EVOS Fluorescent Microscope (Invitrogen). A virus:DMEM dilution that produced approximately 20 infected cells per 10X FOV was used for experiments.

**2.5 Gel electrophoresis of DNA and proteins**

DNA samples were incubated with an equal volume of 5X loading dye. Agarose gels were cast at concentrations ranging from 0.5% to 2% agarose in 1X TAE buffer (40 mM Tris, 20 mM Acetate, 1 mM EDTA) containing ethidium bromide. The DNA samples were then electrophoresed for 45 minutes at 160 volts (V) using the PowerPac Basic Power Supply (Bio-Rad) and visualized under UV light.

Protein samples were added to an equal volume of 2X Laemmli buffer and subsequently boiled for 15 to 20 minutes at 100°C. Polyacrylamide resolving gels were cast at percentages ranging from 10% to 12%. The recipe for a 12% resolving gel is as follows: 375 mM Tris-HCl pH 6.8, 0.1% (v/v) SDS, 0.4% (v/v) Tetramethylethylenediamine (TEMED), 12% (v/v) Acryl/Bis-Acryl, and 0.1% (v/v) APS. A stacking gel (5% (v/v) Acryl/Bis-Acryl, 100 mM Tris-HCl pH 8.7, 0.1% (v/v) SDS, 0.1%(v/v) APS, and 0.4% (v/v) TEMED. The solidified gels were

added to the mini-PROTEAN Tetra Cell (Bio-Rad) and SDS-PAGE running buffer (0.1% SDS, 192 mM glycine, 25 mM Tris pH 9.5) was added. The protein samples were loaded into the wells and were electrophoretically separated for 20 minutes at 80 V (protein stacking) followed by 80 minutes at 120 V (protein separation).

### 2.5.1 Western blotting

Proteins separated by gel electrophoresis (**Section 2.5.1**) were transferred to a nitrocellulose membrane using the iBlot gel transfer device (Invitrogen) according to the manufacturers protocol. Membranes were then blocked with 20 mL PBST buffer (1X PBS and 0.1% Tween-20) containing 5% (w/v) skim milk powder while rocking for 1 hour at room temperature. The membranes were then incubated with one of the following primary antibodies diluted in 10 mL of PBST buffer containing 5% skim milk powder: anti-6XHis (1:10000) (Sigma, St. Louis MO), anti-GST (1:5000) (Sigma), anti-β-actin (1:5000) (Sigma), anti-NusA (1:1000) (Sigma), anti-RSV N (1:1000) (Abcam, Cambridge UK), or anti-RSV P (1:1000) (Abcam). Following an overnight incubation at 4$^{\circ}$C, the membranes were washed 3 times with PBST, and then treated with goat anti-mouse HRP secondary antibody (1:5000) in PBST+5% skim milk powder for 45 minutes while rocking at room temperature. The membranes were washed an additional 3 times with PBST and finally treated with enhanced chemiluminescence solution (ECL) (Pierce, Rockford IL) for detection using X-ray film.

### 2.6 $P_{220-241}$ stability assay

LLC-MK2 cells were seeded in separate 24-well plates at a concentration of $1.5x10^5$ cells/well in 1 mL of DMEM. The cells were allowed to incubate for 24 hours at 37°C and 5% $CO_2$ to adhere to the culture wells. The media was aspirated and the cells were washed twice with sterile 1X PBS before being treated with the purified recombinant $P_{220-241}$ (20 µM) in DMEM or DMEM alone for 0, 1, 4, 8, 24, 48 and 72 hours. At each time point, the respective solutions were aspirated from the culture wells and washed twice with 1 mL of Trypsin-EDTA (to wash off membrane-bound proteins) and then with 1X sterile PBS. The cells were subsequently trypsinized with 400 µL of 0.5 mg/mL Trypsin-EDTA at 37°C and 5% $CO_2$ for 10 minutes. Trypsinized cells were resuspended in 100 µL of 2X Laemmli buffer and analyzed by SDS-PAGE and Western blot with anti-6XHis primary antibody as previously described in **Sections 2.5.1 and 2.5.2**.

### 2.7 Phosphoprotein mimetic inhibition assay: RSV A and B

LLC-MK2 cells were seeded at a concentration of $1.5x10^5$ cells (in 1 mL of DMEM+10% FBS) per shell vial containing microscope cover slips, and were allowed to incubate for 24 hours at 37°C and 5% $CO_2$ to allow the cells to adhere. The medium was aspirated, and the cells were washed twice with 1X sterile PBS. The cells were then pre-treated with either the purified recombinant $P_{220-241}$ (at concentrations of 20 µM, 10 µM, 5 µM and 2.5 µM ) in DMEM, 20 µM of PB1

(negative control peptide) in DMEM , 20 μM of $P_{scram}$ (negative control peptide), or DMEM alone (positive control) for 1 hour at 37°C and 5% $CO_2$. Medium was then aspirated from all shell vials (excluding the no virus control), the cells were washed two times with sterile 1X PBS, and were infected with pre-titered RSV A or RSV B in DMEM at a final volume of 400 μL. All shell vials were centrifuged for 30 minutes at 1,500 x g, followed by a 30 minute incubation period at 37°C and 5% $CO_2$. The viral medium was removed, and the cells were treated with a second round of the purified recombinant proteins or DMEM alone. The final volume of all pre and post-incubation solutions was 400 μL. Cell cultures were allowed to incubate for another 48 hours, and were then stained using DFA reagent as previously described in **Section 2.4.1**. Overall percent inhibition (PI) was calculated by comparing the average number of viruses per 10X field of view (FOV) in the virus only control (V) with the average number of viruses per FOV in each of the peptide treatments (P); (PI=[(V-P)/(V)]x100%).

### 2.7.1 Phosphoprotein mimetic inhibition assay: PIV-2

LLC-MK2 cells were seeded at a concentration of $1.5x10^5$ cells (in 1 mL of DMEM+10% FBS) per shell vial containing microscope cover slips, and were allowed to incubate for 24 hours at 37°C and 5% $CO_2$ to allow the cells to adhere. The medium was aspirated, and the cells were washed twice with 1X sterile PBS. The cells were then pre-treated with either 20 μM of $P_{220-241}$ in DMEM, 20 μM of $P_{scram}$ (positive control peptide), or DMEM alone (negative control) for 1 hour at

37°C and 5% $CO_2$. Medium was then aspirated from all shell vials (excluding the no virus control), the cells were washed two times with sterile 1X PBS, and were treated with pre-titered PIV-2 at a final volume of 400 µL. All shell vials were centrifuged for 30 minutes at 1,500 x g, followed by a 30 minute incubation period at 37°C and 5% $CO_2$. The viral medium was removed, and the cells were treated with a second round of the purified recombinant proteins or DMEM alone. The final volume of all pre and post-incubation solutions was 400 µL. The cells were allowed to incubate for an additional 24 hours, and were then visualized by fluorescence microscopy as previously described in **Section 2.4.1**. Overall PI was calculated as was described in **Section 2.7.1**.

### 2.8 Inhibition of progeny virus release assay

LLC-MK2 cells were seeded at a concentration of $1.5x10^5$ cells (in 1 mL of DMEM+10% FBS) per shell vial containing microscope cover slips, and were allowed to incubate for 24 hours at 37°C and 5% $CO_2$ to allow cells to adhere. The medium was aspirated, and the cells were washed twice with 1X sterile PBS. The cells were then pre-treated with either the purified recombinant $P_{220-241}$ (20 µM), $P_{scram}$ (20 µM), or DMEM alone for 1 hour at 37°C and 5% $CO_2$. Medium was then aspirated from all shell vials (excluding the no virus control), the cells were washed two times with sterile 1X PBS, and were treated with pre-titered RSV A at a final volume of 400 µL. All shell vials were centrifuged for 30 minutes at 1,500 x g, followed by a 30 minute incubation period at 37°C and 5% $CO_2$. The

viral medium was removed, and the cells were treated with a second round of the purified recombinant proteins, or DMEM alone. The final volume of all pre and post-incubation solutions was 400 µL. The cells were allowed to incubate for 48 hours at 37°C and 5% $CO_2$. To measure inhibition of progeny virion release, 200 µL of each of the cell supernatants were collected and added to 200 µL of fresh DMEM media. The respective solutions were added to new shell vials containing confluent monolayers of LLC-MK2 cells, allowed to incubate for 48 hours, and the amount of virus was quantified by fluorescence microscopy as was previously described in **Section 2.4.1**.

### 2.9 Toxicity: cell replication assays

LLC-MK2 and BEAS-2B cells (in separate experiments) were seeded in 24-well plates at a concentration of $1.5x10^5$ cells/well in 1 mL of DMEM+10% FBS. The cells were allowed to incubate for 24 hours at 37°C and 5% $CO_2$ to adhere to the culture wells. The medium was aspirated and the cells were washed twice with 1X sterile PBS before being treated with either 20 µM of purified $P_{220-241}$ in DMEM+10% FBS, 20 µM PB1 in DMEM+10% FBS, DMEM+10% FBS alone, or 2 mg/mL cycloheximide (CH) in DMEM+10% FBS for 0, 8, 24, 48 and 72 hours. A second experiment was conducted where the cells were allowed to incubate for 1 to 7 days. In this case, the cells were treated with a new batch of purified protein every 48 hours. At each of these time points, the respective solutions were aspirated from the culture wells and washed twice with

1X sterile PBS. The cells were subsequently trypsinized with 750 µL of 0.5 mg/mL Trypsin-EDTA at 37°C and 5% $CO_2$ for 10 minutes. Cell density was assessed as previously described by Mohler et al (1996). Briefly, each sample was thoroughly re-suspended before being aliquoted into individual 1 cm spectrophotometer cuvettes, and immediately quantitated by taking absorbance readings (in triplicates) at 800 nm. As a blank, 750 µL of 0.5 mg/ml Trypsin-EDTA was used.

### 2.9.1 Toxicity: adenylate kinase assay

LLC-MK2 or BEAS-2B cells (in separate experiments) were seeded in wells of a 24-well plate at a concentration of $1.5x10^5$ cells/well in DMEM+10% FBS. The cells were allowed to incubate overnight at 37°C and 5% $CO_2$. The wells were washed with sterile 1X PBS before being treated with either 20 µM of purified $P_{220-241}$ in DMEM+10% FBS, 20 µM of PB1 in DMEM+10% FBS, or DMEM+10% FBS alone for 0, 8, 24, 48, or 72 hours. At each of these time points, a control well was treated with 750 µL of lysis buffer (0.1% SDS, 1% Triton X-100). An adenylate kinase release assay was then performed as per the manufacturers protocol (Lonza, Mississauga ON). Aliquots (20 µL) of each cell supernatant were incubated with 100 µL of adenylate kinase detection reagent (Lonza) for 5 minutes. This reaction is a two-step process, which first involves the conversion of ADP to ATP by adenylate kinase. The ATP is then used as an energy source to convert luciferin to oxyluciferin, which in turn releases light.

Relative light units (RLUs) were then measured with 1 second integrated readings (in triplicates) using a 20/20-n Single Tube Luminometer (Promega, Madison WI).

### 2.9.2 Toxicity: RBC lysis assay

Blood was obtained from healthy donors and the samples were subject to a complete blood count (St. Joseph's Hospital, Hamilton, Ontario). Purified RBCs were diluted to $5.0x10^8$ cells/mL in sterile PBS. $P_{220-241}$ (20 μM) in 1X PBS, PB1 (20 μM) in 1X PBS, 1X PBS alone, or lysis buffer (0.1% SDS, 1% Triton X-100) were incubated with the RBCs for 1 to 24 hours at 37°C and 5% $CO_2$. At each of these time points, the cells were centrifuged at 5,000 x g for 5 minutes, and the supernatants were added to separate wells of a 96-well clear-bottom plate. RBC lysis was measured as previously described (Bleumink-Pluym et al, 2013). Absorbance readings (in triplicates) were measured at 420 nm (maximum absorbance of hemoglobin) using a BioTek MicroQuant Plate Reader. Percent lysis was calculated as follows: [(Absorbance – PBS Absorbance)/(Lysis Absorbance – PBS Absorbance)] x100%.

## 2.10 Glutathione S-Transferase (GST) pull-down assays

GST expression plasmids were transformed into *E. coli* BL21 (DE3) or Rosetta (DE3) cells, and cell lysates were obtained as previously described in

**Section 2.2.3**. Magnetic glutathione-agarose beads (Sigma) were washed in 1 mL of PBST buffer and then incubated with *E. coli* cell lysates containing GST-N or GST constructs for 2 hours, while nutating at 4°C. The beads were then washed briefly with PBST before being blocked with 25 mL of PBST+ 5% BSA overnight, while nutating at 4°C. After blocking, the beads were centrifuged at 3000 x g to remove the supernatant. Aliquots of 50 µL of GST-bound beads were mixed with 1 mL of *E. coli* cell lysates containing over-expressed His-tagged proteins and left nutating for 2 hours. The beads were then centrifuged at 16,000 x g for 1 minute, and the supernatant was removed. The remaining pellets were washed 7 times in a high salt wash buffer (20 mM TRIS-HCl pH 7.0, 500 mM KCl, 0.1% Triton X-100). The last wash sample was collected, while the beads were subsequently resuspended in 50 µL of 2X Laemmli buffer and boiled for 15 to 20 minutes. Samples were run on a 12% SDS-PAGE gel and analyzed by Western blot as previously described in **Sections 2.5.1 and 2.5.2**.

### 2.11 I*n vitro* immunoprecipitations

LLC-MK2 cells were seeded in T25 flasks and grown until confluent. RSV was then added to the cells in R-Mix Refeed medium and allowed to incubate for 4 days. For the control N and P antibody immunoprecipitations, the cells were immediately scraped off the monolayer and centrifuged at 14,000 x g for 3 minutes. When performing the anti-His immunoprecipitations, purified $P_{220-241}$ was added to cells at a concentration of 20 µM and allowed to incubate for 24 hours

prior to scraping the cells. Following centrifugation, the cells were resuspended in 500 µL of ice cold lysis buffer (50 mM Tris-HCl pH 7.2, 100 mM KCl, 0.1% SDS, 1% Triton X-100, 1 EDTA-free protease inhibitor) and allowed to nutate for 3 hours at 4°C. The lysed cells were then centrifuged at 14,000 x g for 3 minutes and the supernatant was added to 30 µL of protein A/G agarose beads (Sigma) to pre-clear the lysate. The beads were allowed to nutate at 4°C for 1 hour, were centrifuged at 14,000 x g for 3 minutes, and the supernatant was collected. Primary anti-His, anti-RSV N, or anti-RSV P primary antibodies were then added to make a final dilution of 1:500, and left to nutate overnight at 4°C. To bind the primary antibodies, 30 µL of protein A/G beads was added and left to nutate for an additional hour at 4°C. The bound beads were then washed 2 times with 500 µL of high salt wash buffer (500 mM KCl, 20 mM Tris-HCl pH 7.0, 0.1% Triton X-100) before being centrifuged at 14,000 x g for 3 minutes. The beads were resuspended in 30 µL of 2X Laemmli buffer and boiled for 20 minutes. The samples were then analyzed by SDS-PAGE and Western blot as previously described in **Sections 2.5.1 and 2.5.2**.

### 2.12 Statistical analyses

Results were interpreted using a Student's t-test and a P-value $<0.05$ was considered statistically significant.

# CHAPTER THREE

# RESULTS

## 3.1 – Inhibition of RSV A and B infection *in vitro* using $P_{220-241}$

### 3.1.1 Stability of $P_{220-241}$ within cells

We first investigated whether purified recombinant $P_{220-241}$ was capable of entering LLC-MK2 cells *in vitro.* Peptide therapeutics are often limited by their small size and inability to be taken up by host cells, as such this was a crucial step before testing for RSV inhibition activity. LLC-MK2 cells were seeded in 24-well plates, and then incubated with purified $P_{220-241}$ at a concentration of 20 μM for one of the following time points: 10 minutes, 1 hour, 4 hours, 8 hours, 24 hours, or 72 hours. At each time point, the cells were washed with trypsin to remove any membrane-bound protein, thus ensuring any detected $P_{220-241}$ was intracellular, and the presence of the peptide was determined via anti-His Western blot (**Figure 3.1.1**). $P_{220-241}$ was present in cells from approximately 10 minutes to 48 hours after adding the peptide to the wells. An anti-β-actin antibody was used as a loading control for this experiment. It should also be noted that we have tested for persistent presence of the peptide in between the 48 hour and 72 hour time points, and have yet to detect the presence of the $P_{220-241}$ within LLC-MK2 after this 48 hour period. These data suggests that $P_{220-241}$ is successfully taken up by cells, presumably through its CPP domain.

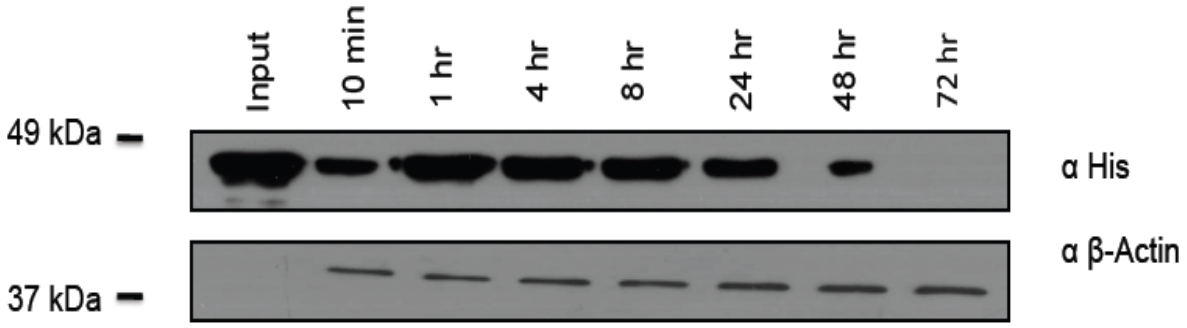


**Figure 3.1.1 $P_{220-241}$ is detectable in cells for 48 hours**
LLC-MK2 cells were incubated with media containing $P_{220-241}$ at concentration of 20 μM. After certain time points, the cells were washed with trypsin, harvested, and analyzed by Western blot. The α-βActin antibody was used as a loading control.

3.1.2 Effects of $P_{220-241}$ on cell replication and growth of RSV A and B

As the central tenant of this project, we hypothesized that purified recombinant $P_{220-241}$ would be capable of inhibiting RSV growth and replication *in vitro*. This was based off previous studies that revealed the C-terminus of the RSV P protein is necessary and sufficient for binding to the RSV N protein, an interaction that is needed to both transcribe and replicate the viral RNA (Garcia-Barreno et, 1996; Tran et al, 2007). Considering that both RSV subtype A and subtype B have been shown to dominate during yearly worldwide epidemics, we thought it was also imperative to test this construct's ability to inhibit replication of both these subtypes. LLC-MK2 cells were seeded in shell vials containing microscope coverslips and pre-incubated with purified $P_{220-241}$ before being treated with RSV (for more details refer to **Section 2.7**). As a positive control, no virus was added to one of the shell vials. As negative controls, an Influenza-

specific PB1 peptide and a scrambled RSV P peptide ($P_{scram}$) were used. $P_{scram}$ is identical to the $P_{220-241}$ construct, however the 21 amino acids of the RSV P domain were randomly scrambled (please refer to **Supplementary Table 5.1** for a description of all protein constructs used in this study). Inhibition of viral infection was calculated following immunofluorescent staining, where RSV-infected cells were stained green by a fluorescein (FITC) –tagged secondary antibody. $P_{220-241}$ (at a concentration of 20 μM) was able to inhibit RSV A replication by an average of 94.8% compared to the virus only control (**Figure 3.1.2A).** The construct also showed inhibition over a range of lower concentrations, including 59.3% at 10 μM, 27.9% at 5 μM, and 10.4% at 2.5 μM. Both negative control peptides (PB1 and $P_{scram}$) did not show any statistically significant reduction in RSV A inhibition (**Figure 3.1.2C**). Very similar results were also obtained when examining cells infected with RSV B (**Figure 3.1.2B**). In a similar pattern to the RSV A data, $P_{220-241}$ displayed inhibition against RSV B over a range of concentrations, with a maximum inhibition of approximately 84% at a concentration of 20 μM. Taken together, these results imply that $P_{220-241}$ is able to successfully reduce RSV replication within infected cells.

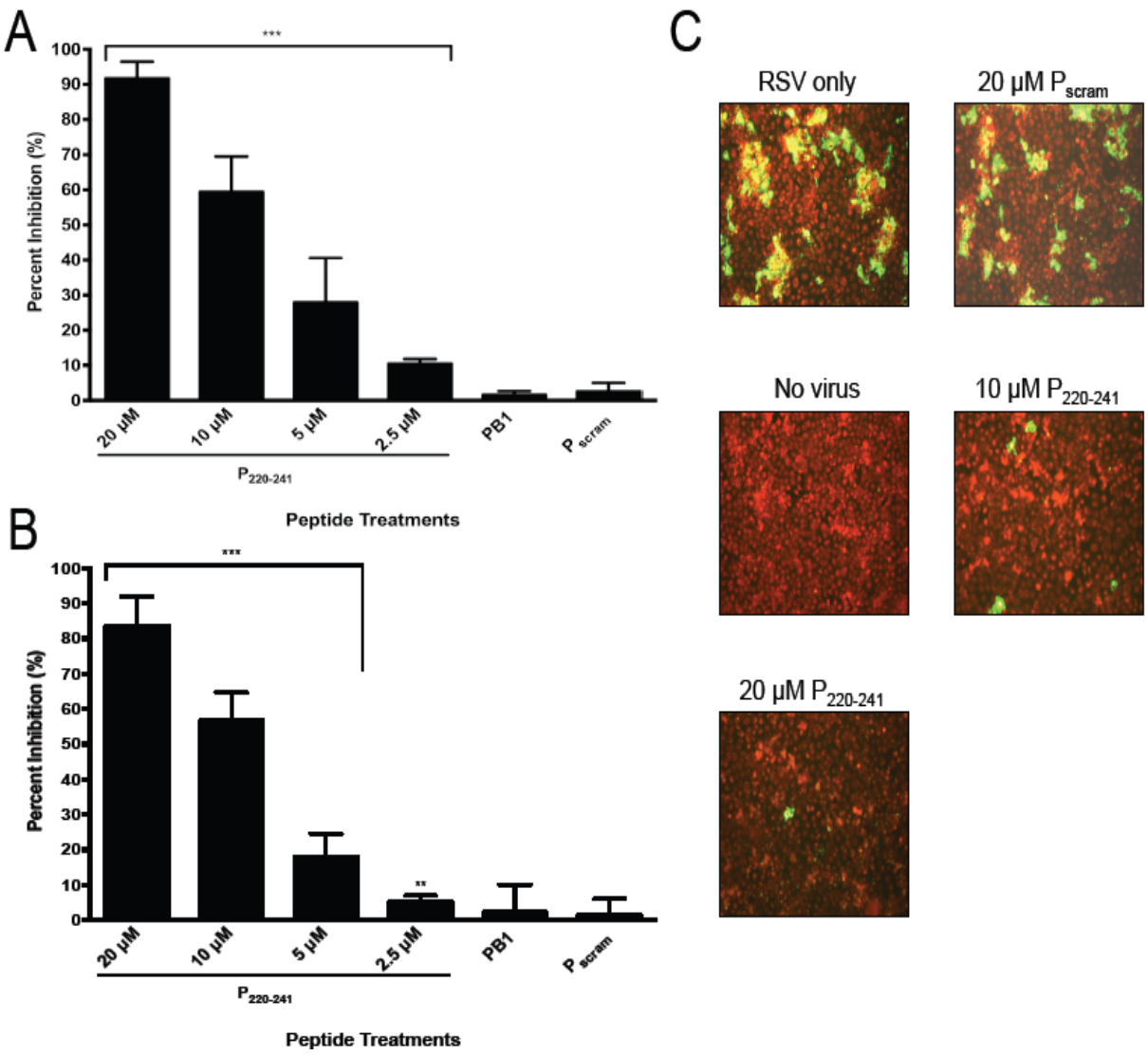


**Figure 3.1.2 $P_{220-241}$ inhibits RSV A and B infection *in vitro***. LLC-MK2 cells were pre-treated with either $P_{220-241}$ in a dose-dependent manner (20 μM-2.5μM), 20 μM of PB1 peptide, or 20 μM of $P_{scram}$, before being infected with RSV A (**panel A**) or RSV B (**panel B**) for 48 hours. The cells were visualized with fluorescence microscopy with virus-infected cells stained green (FITC) and non-infected cells stained red (Evan's blue counterstain) (**Panel C**). Percent inhibition of RSV infection was calculated in reference to the virus only control. The images represent random fields of view. Error bars represent two standard deviations from the mean of 3 independent experiments. ***=P<0.001 **=P<0.05

### 3.1.3 Effect of $P_{220-241}$ on cell replication and growth of PIV-2

Despite the ability of $P_{220-241}$ to inhibit RSV infection *in vitro*, it was still necessary to confirm that $P_{220-241}$ was not acting as a pathogen-associated molecular pattern (PAMP), which could have triggered a host-cell antiviral response towards RSV. To investigate this possibility, we obtained a strain of human parainfluenza virus type 2 (PIV-2), which is also a member of the *Paramyxoviridae* family of viruses. LLC-MK2 cells were seeded in shell vials and treated with purified $P_{220-241}$ at a concentration of 20 μM. The cells were then infected with PIV-2 and later stained in an identical fashion to the LLC-MK2 cells used in the RSV inhibition experiments (for details please refer to **Section 2.7.1**). As displayed in **Figure 3.1.3** below, compared to the virus-only control, $P_{220-241}$ did not show any statistically significant reduction of PIV-2 infection. The percent inhibition of PIV-2 infection is also displayed next to the inhibition of RSV subtype A infection for ease of comparison. This result suggests that previous RSV inhibition by $P_{220-241}$ displayed in **Figure 3.1.2** was not an artifact of a host-cell antiviral response triggered by a PAMP.

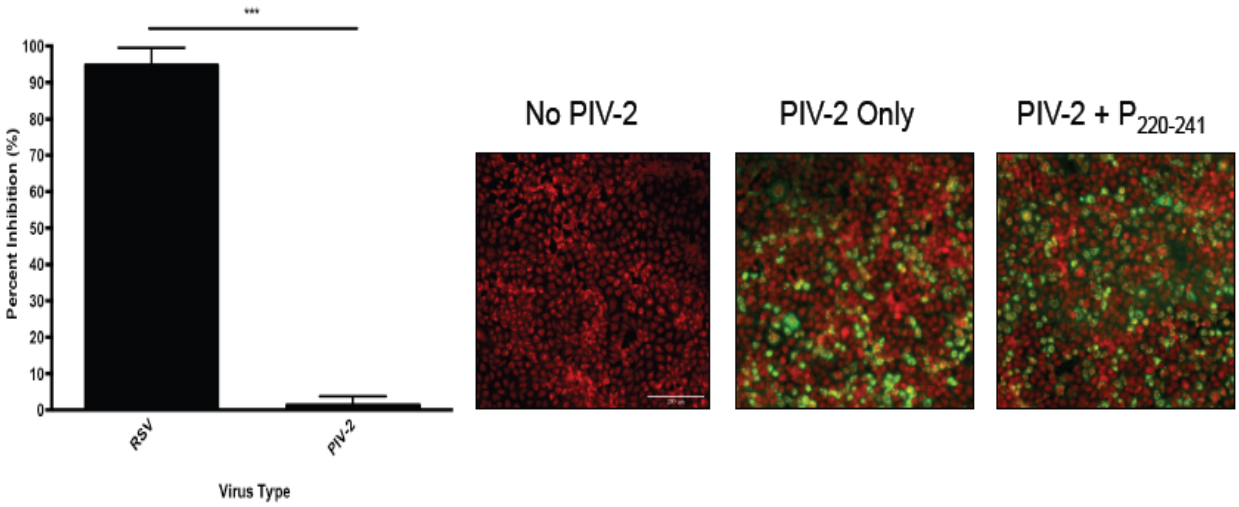


**Figure 3.1.3 $P_{220-241}$ does not inhibit PIV-2 infection *in vitro*.**
LLC-MK2 cells were pre-treated with 20 µM of purified $P_{220-241}$ prior to being infected with PIV-2. The cells were visualized at 10X magnification with PIV-2 cells stained green (FITC) and non-infected cells stained red (Evan's blue counterstain). Percent inhibition was calculated and compared to RSV-infected cells treated with 20 µM of $P_{220-241}$ . The images represent random fields of view. Error bars represent two standard deviations from the mean of 3 independent experiments. ***=P<0.001

### 3.1.4 Effect of $P_{220-241}$ on progeny RSV virus production

Our previous RSV inhibition data demonstrated that purified $P_{220-241}$ could inhibit RSV replication within cells. However, this data did not confirm that the peptide could inhibit release of progeny RSV virions into the surrounding medium. To investigate this question, shell vials were infected with RSV and then treated with either $P_{220-241}$ (20 µM), control peptide $P_{scram}$ (20 µM), RSV alone, or media alone, using the same infection protocol. However, following the 48-hour infection, samples of the cell supernatant were taken to infect new shell vials. The cells were visualized by fluorescent microscopy, and the average number of

infected cells per 10X FOV was quantified (**Figure 3.1.4**). Compared to an average of just less than 1 infected cell per 10X FOV in $P_{220-241}$ treated cells, there was an average of 9.4 infected cells per 10X FOV for those treated with RSV alone (approximately 92% inhibition). This reduction in viral load signifies that not only does $P_{220-241}$ prevent efficient intracellular replication of RSV, but it also helps to disrupt efficient release of new progeny virus.

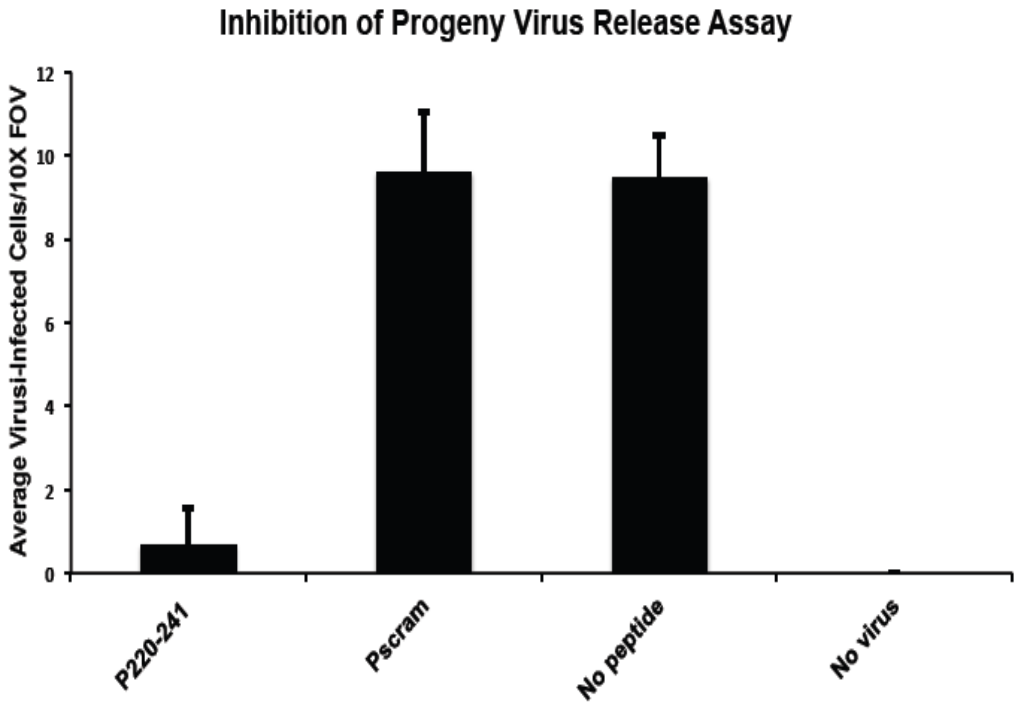


**Figure 3.1.4 $P_{220-241}$ inhibits release of progeny RSV virions *in vitro***. LLC-MK2 cells were treated with either $P_{220-241}$ at a concentration of 20 µM, 20 µM of $P_{scram}$, RSV alone, or cell media alone. After adding RSV to corresponding cells, they were allowed to incubate for 48 hours. A sample of the cellular supernatant was then taken to infect new confluent cells for an additional 48 hours. The cells were visualized with fluorescence microscopy and the average number of viruses per 10X FOV was calculated and graphed above. Error bars represent two standard deviations from the mean of 3 independent experiments.

## 3.2 – Cytotoxic effects of $P_{220-241}$ *in vitro*

### 3.2.1 Effect of $P_{220-241}$ on cell replication

To confirm that the previously aforementioned RSV inhibition data was not an indirect bi-product of cellular toxicity, we used a series of different assays. Firstly, direct visual analysis of cells exposed to 20 μM of purified $P_{220-241}$ did not show any apparent morphological changes in cell structure (data not shown). To further substantiate this claim, a cell replication assay was performed using two different cell lines: LLC-MK2 and BEAS-2B cells. LLC-MK2 or BEAS-2B cells were seeded in shell vials, and were then treated with one of the following conditions: 20 μM of $P_{220-241}$, 20 μM of PB1 negative control peptide, 2 mg/mL cycloheximide (CH), or medium alone. CH is a potent inhibitor of protein synthesis and cell growth in eukaryotic cells, and thus was used as a positive control in this experiment. Over a series of time intervals (0 hours to 72 hours), the cells were washed, and their absorbance was measured at 800 nm, providing a reading directly proportional to cell density (Mohler et al, 1996). There was no statistically significant difference in absorbance readings between $P_{220-241}$, control PB1 peptide, or medium-only treated cells. Cells treated with CH showed a relatively constant absorbance reading over the entire experiment. Results for this cell replication assay are represented graphically in **Figure 3.2.1A**. To further substantiate this data, we have also achieved similar results using a Prestoblue cell replication assay, which measures cell density as a function of relative

fluorescence (**Supplementary Figure S2**).

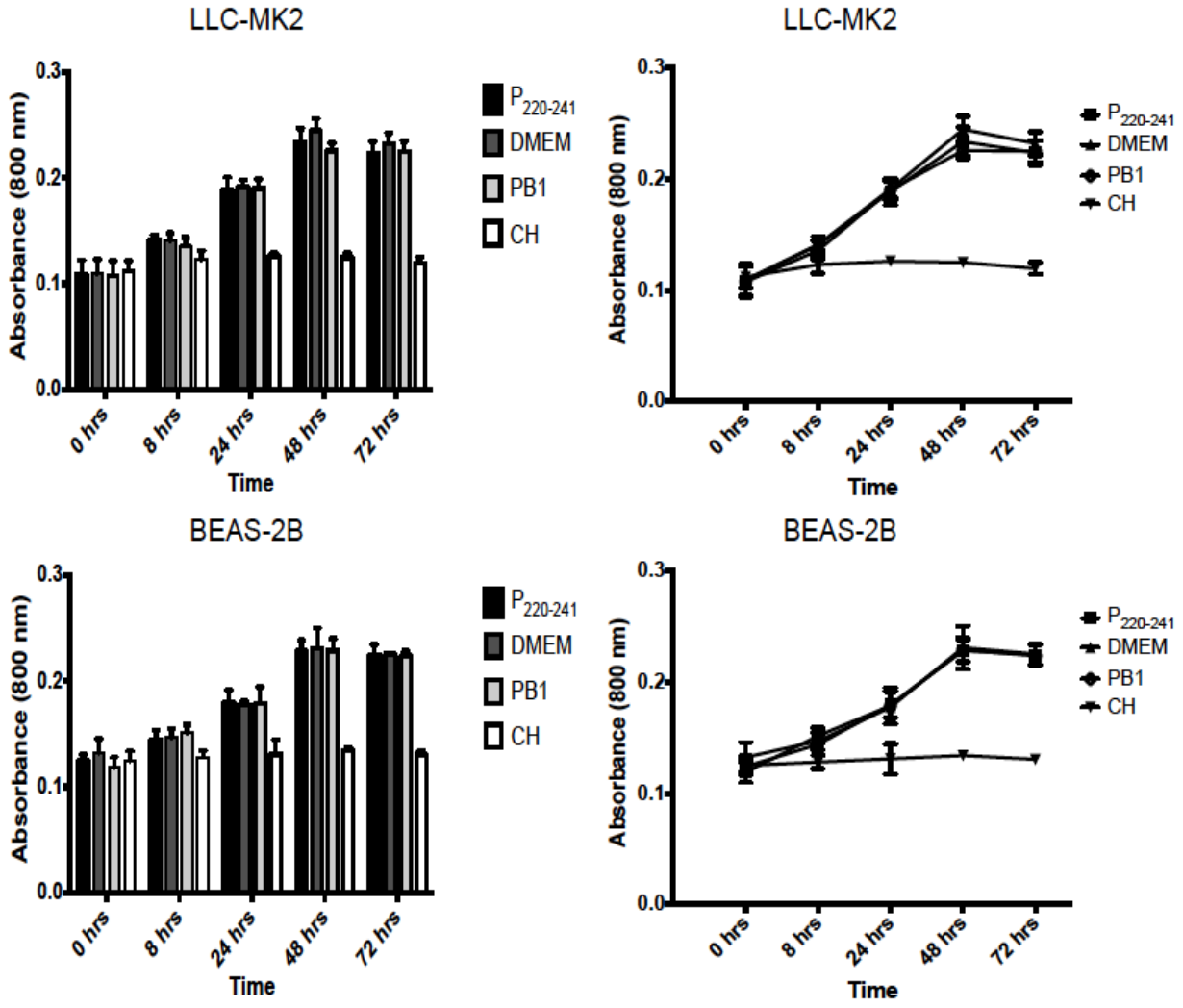


**Figure 3.2.1A Single dose of $P_{220-241}$ does not inhibit cell replication *in vitro***
LLC-MK2 and BEAS-2B (in separate experiments) were seeded in shell vials and treated with one of the following: 20 μM $P_{220-241}$, 20 μM control peptide, cell media alone (DMEM), or 2 mg/mL cycloheximide in cell media. The cells were harvested at various time points, and cell replication was quantified by absorbance at 800 nm. Error bars represent two standard deviations from the means of 3 independent experiments.

We also wanted to investigate whether $P_{220-241}$ displayed any toxic effects on cells when multiple doses were given over a prolonged period of time. This scenario may be more indicative of a true clinical scenario, where cells would constantly be exposed to the peptide for a longer duration of time. LLC-MK2 cells were seeded in shell vials, and where then treated with one of the following conditions: 20 μM of $P_{220-241}$, 20 μM of PB1 negative control peptide, 2 mg/mL CH, or medium alone. Since our previous half-life data (**Figure 3.1.1**) indicated that $P_{220-241}$ was stable in cells for approximately 48 hours, we took this into account and replaced the peptide and medium solutions every 2 days. At 24-hour intervals over a period of 7 days, the cells were washed, and the absorbance was measured at 800 nm. Similar to previous results, there was no statistically significant difference in absorbance readings between $P_{220-241}$, control peptide, or medium-only treated cells (**Figure 3.2.1B**). In combination with previous data outlined in **Figure 3.2.1A**, these results suggest that $P_{220-241}$ does not negatively affect cell replication *in vitro*.

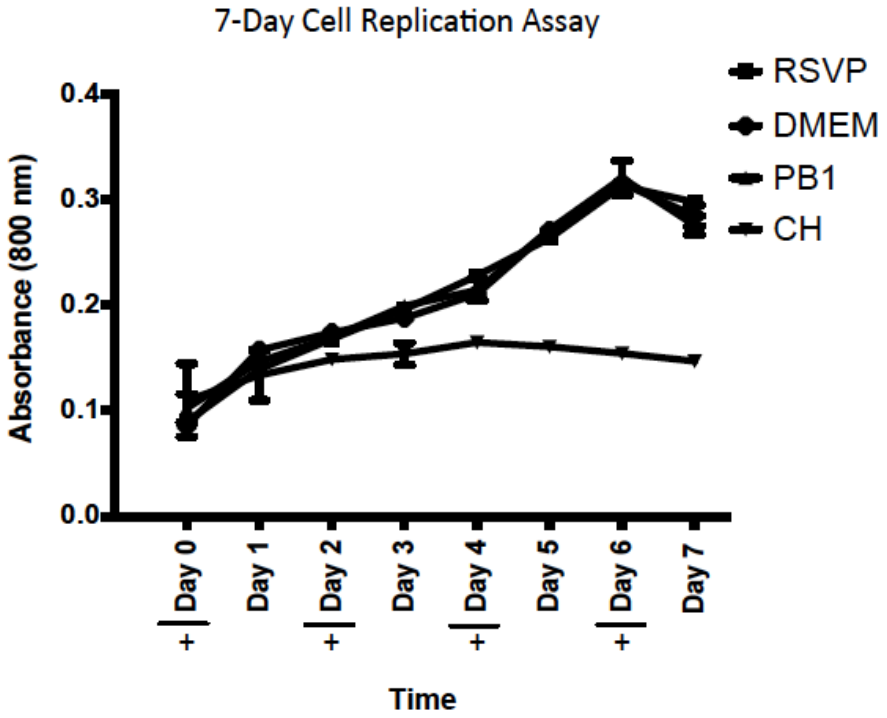


**Figure 3.2.1B Multiple doses of $P_{220-241}$ does not affect cell replication over 7 days**
LLC-MK2 cells were seeded in shell vials and treated with one of the following: 20 μM $P_{220-241}$, 20 μM control peptide, cell media alone (DMEM), or 2 mg/mL cycloheximide in DMEM. The cells were harvested at various time points over a period of 7 days, and cell replication was quantified by absorbance at 800 nm. To account for protein degradation, the cells were re-treated with new peptide every 48 hours (addition of new peptide represented by "+"). Error bars represent two standard deviations from the means of 3 independent experiments.

### 3.2.2 Effect of $P_{220-241}$ on adenylate kinase release from cells

We next investigated toxicity of $P_{220-241}$ using a well-known commercial assay (Lonza), which measures release of adenylate kinase into the extracellular medium. Adenylate kinase is a prominent phosphotransferase enzyme present in all eukaryotic cells, and it is released into the extracellular medium upon cell death. LLC-MK2 or BEAS-2B cells were seeded in shell vials, and then treated with one of the following conditions: 20 μM of $P_{220-241}$, 20 μM of PB1 negative

control peptide, lysis buffer (positive control), or medium alone. At the appropriate time point (0 hours, 8 hours, 24 hours, 48 hours, or 72 hours), a sample from the cell supernatant was taken and incubated with adenylate kinase detection reagent. Incubation with this reagent produces a bioluminescent signal, which can be quantified in relative light units (RLUs). Lysis buffer was used as a positive control as the cells were fully lysed, resulting in comparatively high RLU values. Relative bioluminescence produced by the presence of $P_{220\text{-}241}$ was comparable to that of control conditions, and was significantly different from when the cells were treated with lysis buffer alone (**Figure 3.2.2**). This signifies that exposure of cells to $P_{220\text{-}241}$ likely does not alter membrane integrity *in vitro*.

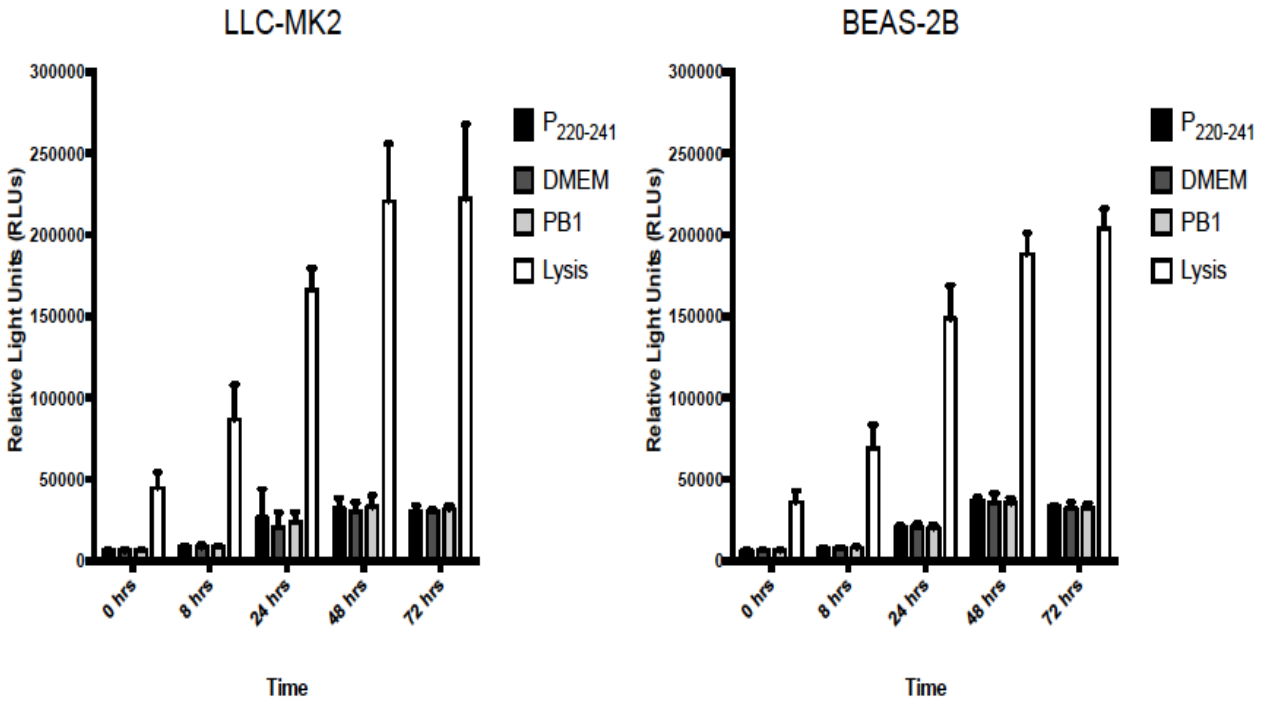


**Figure 3.2.2 $P_{220-241}$ does not cause cellular lysis in LLC-MK2 or BEAS-2B cells**
LLC-MK2 and BEAS-2B (in separate experiments) were seeded in shell vials and treated with one of the following: 20 μM $P_{220-241}$, 20 μM control peptide, cell media alone (DMEM), or 0.1% Triton X-100 lysis buffer. Aliquots of the cell supernatants were harvested at various time points, and levels of adenylate kinase were quantified in Relative Light Units (RLUs) using a bioluminescent luciferase reaction. Error bars represent two standard deviations from the mean of three independent experiments.

### 3.2.3 Effect of $P_{220-241}$ on red blood cell lysis

In order to provide a final measure of toxicity, the effect of $P_{220-241}$ on the cell membrane was further assessed using a RBC lysis assay. RBCs from healthy donors were harvested, purified and incubated with one of the following treatments: 20 μM $P_{220-241}$ in 1X PBS, 20 μM PB1 negative control peptide in 1X PBS (20 μM), 1X PBS alone, or lysis buffer (positive control). After either 1 hour

or 24 hours, an aliquot of the cell supernatant was collected and an absorbance measurement at 420 nm was taken (420 nm corresponds to the maximum absorbance of hemoglobin). Percent lysis was calculated (see **Section 2.9.2** for details) and graphed below in **Figure 3.2.3**. Compared to PBS buffer alone and control PB1 peptide, $P_{220-241}$ displayed negligible absorbance readings, thereby suggesting that $P_{220-241}$ does not lyse RBCs *in vitro*.

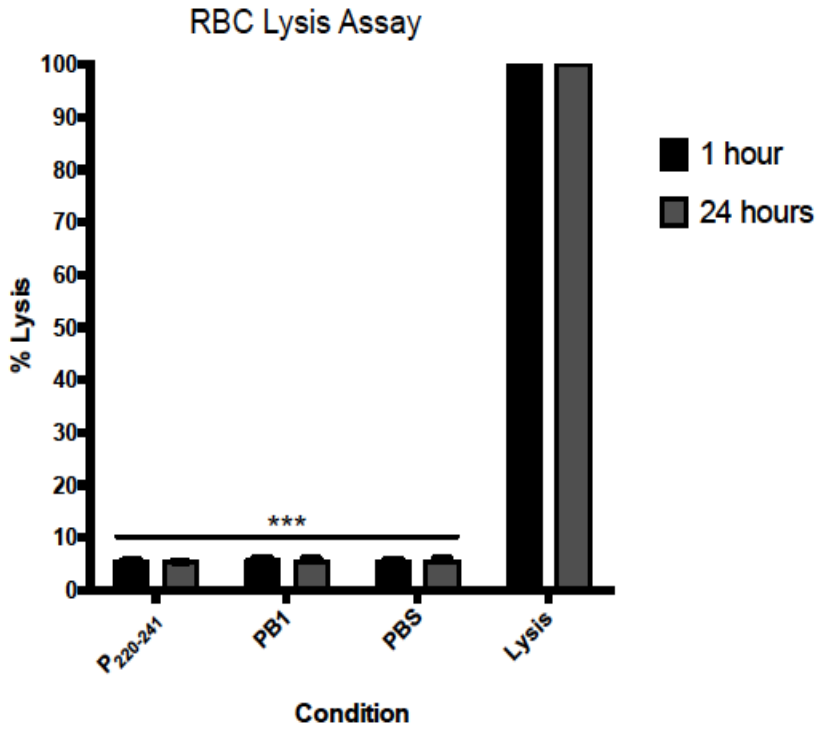


**Figure 3.2.3 $P_{220-241}$ does not cause RBC lysis *in vitro***
Toxicity was measured by treating purified RBCs with $P_{220-241}$, PB1 control peptide, PBS alone (negative control), or lysis buffer (positive control) and measuring the absorbance of RBC supernatants at a wavelength of 420 nm. Percent lysis was calculated in reference to the lysis buffer control (see methods). Error bars represent two standard deviations from the mean of 3 independent experiments. ***=$p<0.001$

## 3.3 – Mimetic mechanism of action: GST pull-down experiments

### 3.3.1 – Interaction between $P_{220-241}$ and GST-N *in vitro*

As previously mentioned, several studies have reported that the C-terminus of RSV P protein binds to the RSV N protein (Garcia-Barreno et al, 1996; Tran et al, 2007). Therefore, we hypothesized that the $P_{220-241}$ mimetic should bind in a similar fashion to the N protein. To investigate this potential interaction, we designed a series of recombinant proteins to use in GST pull-down experiments (refer to **Supplementary Table 5.1** for a list of these constructs). The bait proteins (bound to glutathione-agarose beads) for these experiments were GST-N and GST alone, while the prey proteins were HisNusA-P, HisNusA, $P_{scram}$, and $P_{220-241}$ (**Figure 3.3.1C**). Like MBP, NusA is an *E. coli* protein often used as a carrier molecule to enhance protein half-life and solubility (Nallamsetty and Waugh, 2006). The His-tagged prey proteins were loaded on a gel and analyzed by Western blot as a control to compare their respective sizes, as is seen in the left panel of **Figure 3.3.1A**. After the bait constructs were bound to glutathione-agarose beads, the beads were incubated with one of the four prey constructs. Following washing with high salt buffer, the samples were electrophoretically separated and analyzed by Western blot. GST-N was able to pull-down both $P_{220-241}$ and HisNusA-P, as is displayed in the middle panel of **Figure 3.3.1A**. However, GST-N did not interact with either of the control

constructs (HisNusA and $P_{scram}$). GST alone did not interact with any of the constructs, as is seen in the right panel of **Figure 3.3.1A**. Collectively, this data suggests that not only do HisNusA-P and $P_{220-241}$ copurify with GST-N, but that this interaction is guided by the P protein domain found in each of these protein constructs.

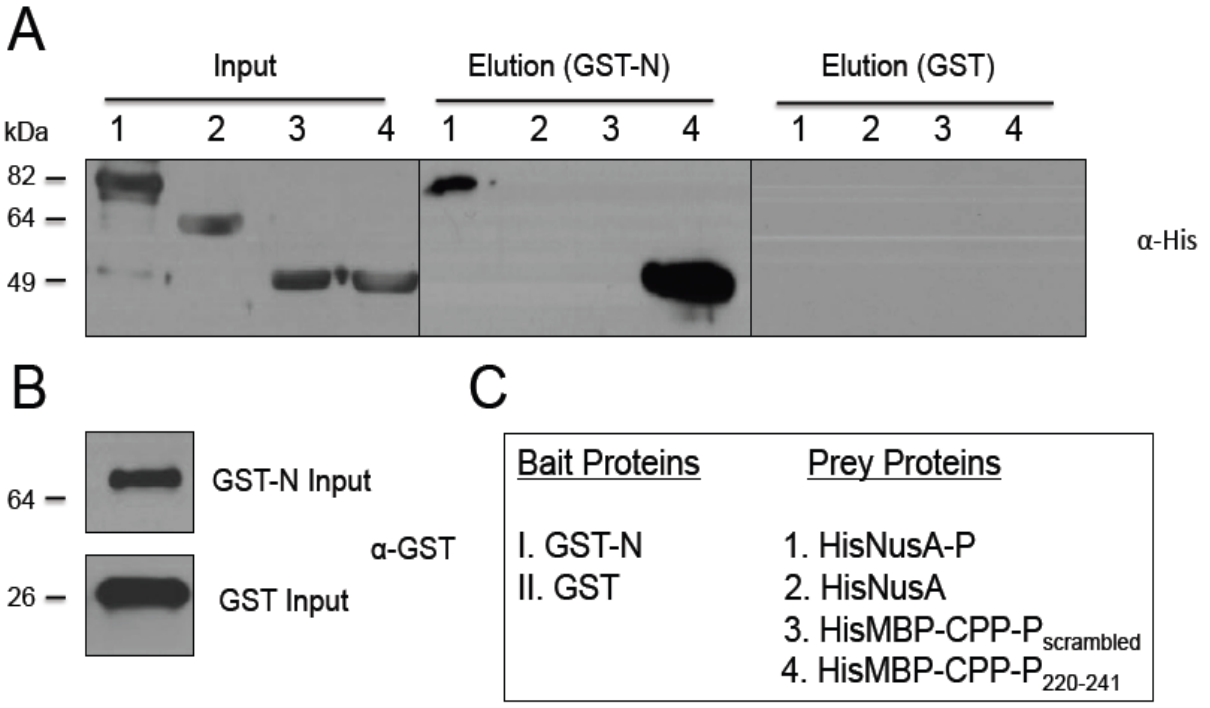


**Figure 3.3.1 $P_{220-241}$ binds to GST-N *in vitro***
*E. coli* cell lysates of GST-N or GST (bait proteins) were incubated with magnetic glutathione-agarose beads. The bound beads were then allowed to incubate with *E. coli* cell lysates containing one of four prey proteins, and then analyzed by Western Blot. **(A)** Input prey proteins (left) and elution fractions from both GST-N and GST-bounds beads. **(B)** Soluble GST-tagged proteins. **(C)** Bait and prey proteins used in the GST pull-down.

### 3.3.2 – $P_{220-241}$ blocks binding of full-length P protein to GST-N *in vitro*

Considering we originally hypothesized that $P_{220-241}$ would likely function by blocking the binding of full-length P protein to N protein, a second GST pull-down assay was used to evaluate this possibility (full-length P protein represented by HisNusA-P; N protein represented by GST-N). The glutathione beads were bound by GST-N and then pre-incubated for 2 hours with $P_{220-241}$ lysate. Following this incubation period, the $P_{220-241}$ lysate was removed and replaced with an equal volume of HisNusA-P lysate. The samples were then once again washed and analyzed by SDS-PAGE and Western blot. Half of the sample was probed with anti-NusA antibody to detect the presence of HisNusA-P, while half the sample was probed with anti-His antibody to detect $P_{220-241}$. While there was a clear detection of His-tagged $P_{220-241}$ (right panel of **Figure 3.3.2**), HisNusA-P was not detected by Western Blot (left panel of **Figure 3.3.2**). This result suggests that $P_{220-241}$ is capable of preventing the association between full-length RSV P and N proteins *in vitro*.

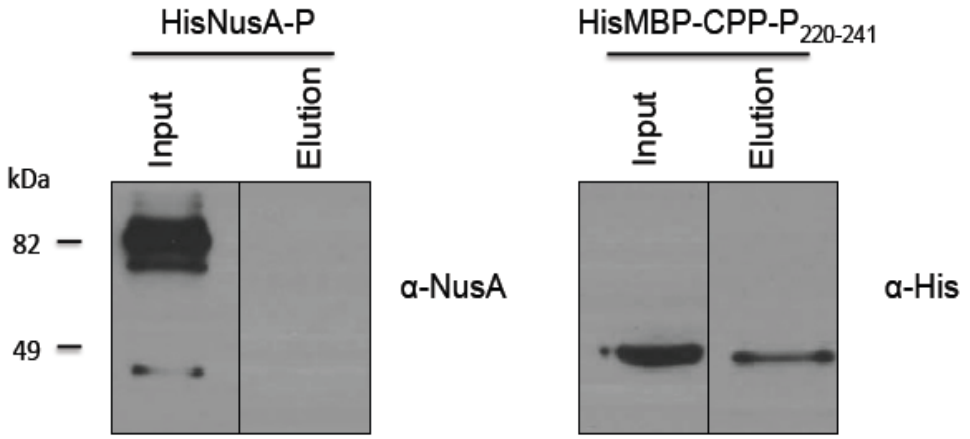


**Figure 3.3.2 $P_{220-241}$ blocks binding of full-length P *in vitro***
*E. coli* cell lysates containing recombinant GST-N were incubated with magnetic glutathione-agarose beads. The bound beads were then pre-incubated with $P_{220-241}$ for 2 hours. The $P_{220-241}$ lysate was then removed, and the beads were incubated with HisNusA-P for an additional 2 hours. Equal amounts of the beads were aliquoted, resuspended in loading buffer, and analyzed by Western blot. Anti-NusA primary antibody was used to detect the presence of HisNusA-P (left), while anti-His primary antibody was used to detect $P_{220-241}$ (right).

## 3.4 – Mimetic mechanism of action: Immunoprecipitation experiments

### 3.4.1 – Immunoprecipitation of N, P, and $P_{220-241}$

While we were able to show that $P_{220-241}$ is capable of binding GST-N and subsequently disrupt the N-P protein interaction *in vitro* using GST pull-down experiments (see above), we next explored this interaction using more robust *in vitro* immunoprecipitation assays involving N and P proteins synthesized by RSV-infected cells. LLC-MK2 cells were infected with RSV and later lysed at 4 days post-infection. The RSV P protein, N protein, and His-tagged $P_{220-241}$ were then immunoprecipitated using anti-P, anti-N, and anti-His primary antibodies,

respectively. The antibodies (now interacting with their targets) were then bound to protein A/G beads and washed with high salt buffer before being loaded onto a protein gel for analysis. Based off the presence of bands corresponding to the N protein, P protein, and His-tagged $P_{220-241}$ proteins, it is clear that each of these respective targets were successfully precipitated from RSV-infected cell lysates. Immunoprecipitation of the each target protein is displayed below in **Figure 3.4.1** following SDS-PAGE and Western blot analysis. A sample of the LLC-MK2 cell lysate was run to show that the target proteins were successfully precipitated from this solution, and a sample of the protein A/G beads was loaded as a control for non-specific binding.

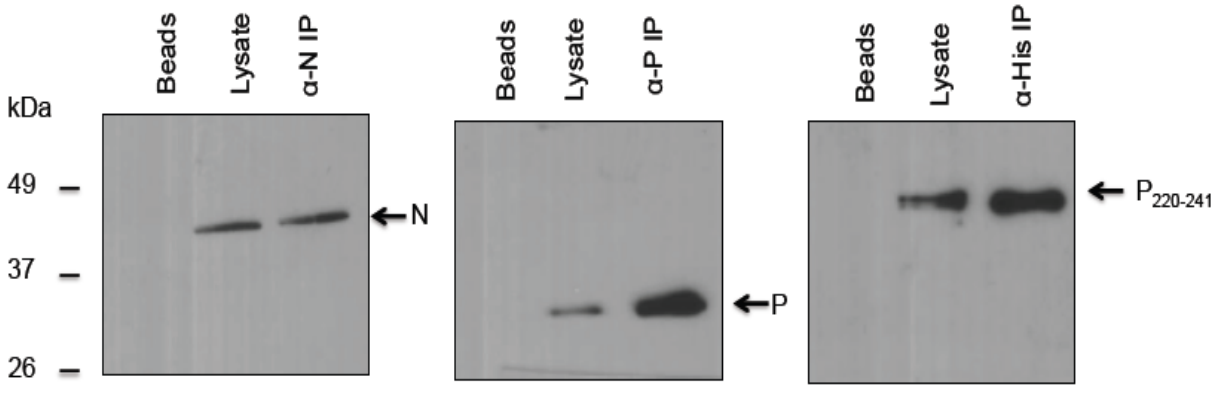


**Figure 3.4.1 Immunoprecipitation using anti-N, anti-P, and anti-His antibodies**
LLC-MK2 cells were infected with RSV and treated with purified $P_{220-241}$. The cells were then lysed and treated with one of the following primary antibodies: anti-N, anti-P, or anti-His. Following immunoprecipitation, the samples were analyzed by SDS-PAGE and Western blot. A sample of lysate was loaded to show the proteins were successfully precipitated, and an aliquot of Protein A/G beads was loaded as a control for non-specific binding.

### 3.4.2 – Co-immunoprecipitation of $P_{220\text{-}241}$ with N alone

Following successful immunoprecipitation of target proteins, we wanted to further our understanding of the mechanism of action of $P_{220\text{-}241}$. To confirm the interaction between the N and P proteins *in vitro*, we immunoprecipitated the RSV N and P proteins individually, and then probed for both N and P proteins following SDS-PAGE and Western blot (**Figure 3.4.2A**). In each case, both the N and P proteins were detected by Western blot, thereby indicating they had co-immunoprecipitated from infected cells. This result implies the N and P proteins were interacting together within RSV-infected cells, as is supported by numerous previous studies (Garcia-Barreno et al, 1996; Tran et al, 2007). Lastly, we investigated whether purified $P_{220\text{-}241}$ could once again disrupt this N-P protein interaction. Following pre-treatment with $P_{220\text{-}241}$, the RSV-infected cells were lysed, and the lysate was then subjected to an anti-His immunoprecipitation. When this sample was later separately probed for either RSV N protein, P protein, or His-tagged $P_{220\text{-}241}$ proteins by Western blot, only full-length RSV P protein was not detected (**Figure 3.4.2B**). Not only does this data support previous results obtained from GST pull-down experiments, but it also suggests that $P_{220\text{-}241}$ is able to successfully interact with RSV N protein within infected cells. Furthermore, the fact that full-length P protein was not detected by Western blot suggests that $P_{220\text{-}241}$ may successfully disrupt proper formation of the RSV RdRp complex *in vitro*.

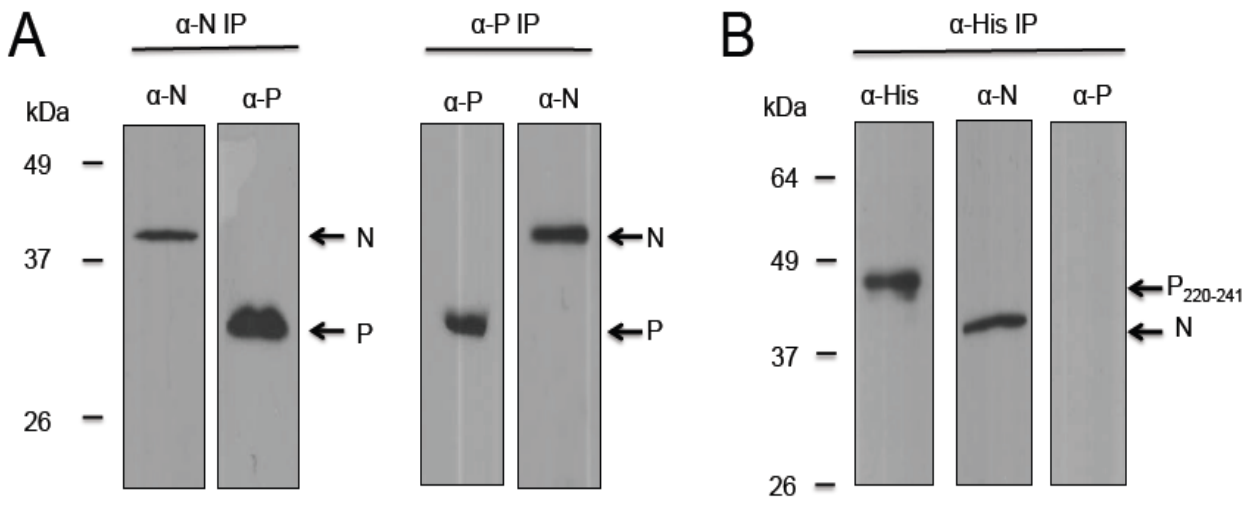


**Figure 3.4.2 $P_{220-241}$ blocks binding of RSV P to N in cell culture.**
(A) Co-immunoprecipitation of RSV N and P using both anti-N (left) and anti-P (right) antibodies, followed by both anti-N and anti-P Western blot. (B) Immunoprecipitation of $P_{220-241}$ (anti-His), with anti-His, anti-N, and anti-P Western blot. The antibodies used for Western blots are listed below the line indicating which antibodies were used for immunoprecipitation (IP).

# CHAPTER FOUR

# DISCUSSION

## 4.1 $P_{220-241}$ is stable within cells *in vitro*

While translocation through the plasma membrane has continuously been deemed as a major limiting step in the delivery of therapeutic macromolecules, we have overcome this dilemma through the use of a CPP domain. Results displayed in **Section 3.1** demonstrate that by fusing a CPP to a chimeric protein, the final protein construct, $P_{220-241}$, is successfully targeted for uptake within cells *in vitro*. We have shown that $P_{220-241}$ is quickly taken up by cells within approximately 10 minutes, and can still be detected by anti-His Western blot following 48 hours of incubation time. These results support previous data from the Mahony laboratory, which showed the efficient targeting of chimeric proteins into HeLa cells to inhibit *C. pneumonia* infection (Stone et al, 2011). There has been a significant amount of debate surrounding the exact mechanism employed by the CPP domain to facilitate entry into cells. While some research supports direct interaction and translocation across the cell membrane, there is also sufficient evidence to support internalization via endocytosis (Bechara and Sagan, 2013; Drin et al, 2003; Richard et al, 2003). In support of the later, Drin et al previously demonstrated that several different cationic CPPs can be taken up by cells, and subsequently accumulate in vesicular structures (Drin et al, 2003). Both clathrin-mediated endocytosis along with calveolae-facilitated uptake have also been described as possible endosomal uptake pathways (Saalik et al, 2004;

Ferrari et al, 2003). Unfortunately, there have been several studies which also seem to contradict these results (Kaplan et al, 2005, Ter-Avetisyan et al, 2009). To support direct translocation across the membrane, the most common theory is such that primarily positively charged cationic CPPs, like the one used in this study, directly translocate across the membrane through interaction with negatively charged residues on the lipid bilayer (also known as "adaptive translocation") (Bechara and Sagan, 2013; Herce and Garcia, 2007). In this model, positively charged residues interact with negatively charged phosphate groups on the extracellular surface of the cell (Bechara and Sagan, 2013; Herce and Garcia, 2007). The CPP becomes attracted to additional positive residues on the opposite side of the lipid bilayer (the intracellular side), which facilitates the translocation process (Herce and Garcia, 2007). As the protein passes through the bilayer, it becomes saturated with water molecules (Herce and Garcia, 2007). This process helps saturate the proteins' charged groups as it passes through the bilayer (Herce and Garcia, 2007). It should also be noted that while this is the most common theory used to explain direct translocation across the membrane, several others have been suggested. A schematic diagram displaying this direct translocation mechanism, along with other possible translocation routes, is displayed below in **Figure 4.1**. While it is difficult to discern the mechanism of cellular entry, it is plausible that there may be more than one possible uptake pathway depending on the nature of the CPP, the type of cells being used, as well as other external factors.

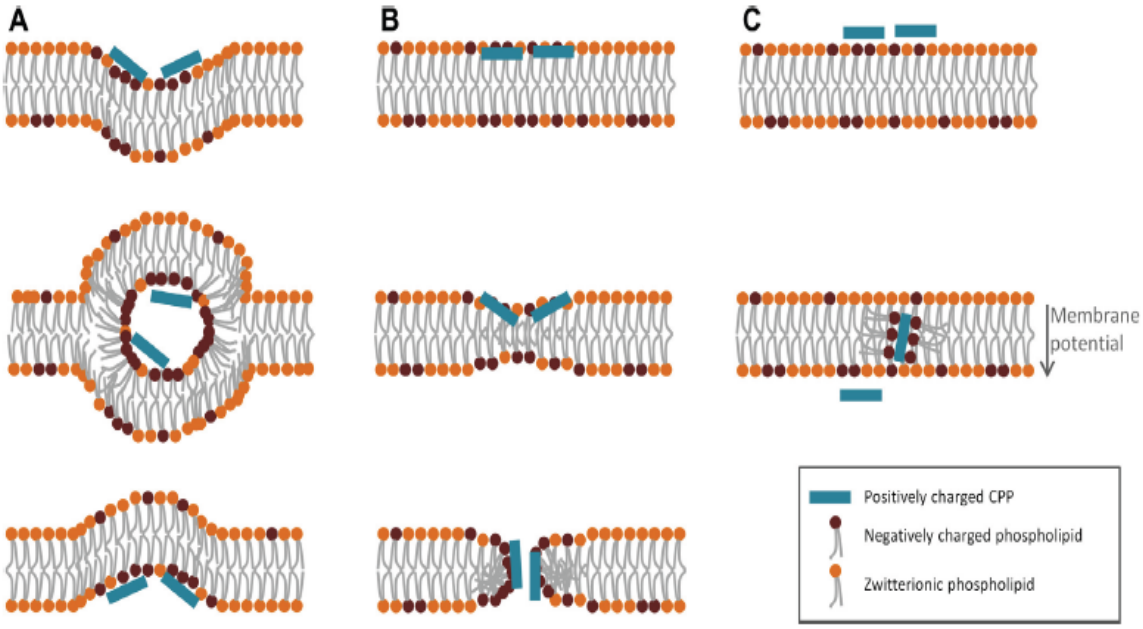


**Figure 4.1 Possible mechanisms of CPP direct cell entry**
The above figure represents several proposed mechanisms for direct entry of CPPs across the outer cell membrane: **(A)** Inverted micelle formation **(B)** Pore formation **(C)** Adaptive translocation. This figure it taken from Bechara and Sagan, 2013.

## 4.2 Inhibition of RSV replication using purified $P_{220-241}$

Following confirmation of entry within cells, we assessed the antiviral activity of purified $P_{220-241}$. As a negative control for this experiment, we successfully cloned a chimeric protein construct identical to $P_{220-241}$, but with the final 21 C-terminal amino acids of the RSV P protein randomly scrambled ($P_{scram}$). We showed that treating LLC-MK2 cells with low micromolar concentrations (20 μM to 2.5 μM) of $P_{220-241}$ was able to inhibit RSV infection by as much as 95%. On the contrary, the $P_{scram}$ negative control peptide showed no statistically significant inhibition of RSV infection ($p>0.05$) at a concentration of 20 μM. Taken

together, this result confirms that the critical anti-RSV activity of the $P_{220-241}$ mimetic is dependent on the primary amino acid sequence of the P protein domain, rather its total charge. Such a result also confirms the specificity of the C-terminus of the P protein for the N protein, as has been previously described in several studies (Garcia-Barreno et al, 1996; Tran et al, 2007). We confirmed this finding by demonstrating that purified $P_{220-241}$ reduced the amount of progeny virus being released into the cellular supernatant by approximately 92%, compared to cells treated with RSV alone. This implies that the mimetic is also able to prevent the release of progeny virions from RSV-infected cells. Despite these promising results, we wanted to rule out the possibility that $P_{220-241}$ was acting as a PAMP and triggering a host-cell antiviral response. To investigate this possibility, we showed that 20 μM of $P_{220-241}$ did not inhibit the replication of PIV-2 within LLC-MK2 cells. While PIV-2 originates from the same *Paramyxoviridae* family of viruses as RSV, $P_{220-241}$ treatment failed to result in any statistically significant reduction in RSV infection. This result implies that the reduction of RSV viral load *in vitro* was not a secondary response to intracellular PAMP-associated antiviral signalling pathways.

When comparing the inhibitory activity of $P_{220-241}$ towards both RSV subtype A and B, the percent inhibition of RSV infection was slightly lower for RSV B strains. The fact that $P_{220-241}$ seems to inhibit RSV A slightly more efficiently than RSV B may be attributed to minor amino acid differences in the C-termini of P in these different subtypes. **Supplementary Table 5.2** shows the

primary amino acid sequences of the final 21 amino acids of RSV P from several different strains of RSV A and B. When comparing between strains within each of the subtypes, there is a 100% similarity in amino acid sequences. However, when comparing between the two subtypes, there is minor differences in their respective amino acid sequences (76% identity). Considering the $P_{220-241}$ peptide mimetic was originally designed using the P protein sequence from a RSV subtype A, it is not a surprise that $P_{220-241}$ was slightly less effective at inhibiting RSV subtype B.

### 4.3 $P_{220-241}$ is non-toxic towards multiple cell lines *in vitro*

By visually observing cells exposed to purified $P_{220-241}$ *in vitro*, there were no noticeable morphological changes to cell structure, compared to control treated cells. Nevertheless, it was imperative to rule out the possibility that the antiviral effects of $P_{220-241}$ were not resultant from cellular toxicity and the subsequent inability of RSV to replicate. To rule this out, we used a series of different cellular toxicity assays. Firstly, cellular replication in the presence of $P_{220-241}$ was unaffected for up to 7 days, assessed by taking absorbance readings at 800 nm. Absorbance readings at this specific wavelength correspond directly to the number of intact cells in suspension, and these readings are also unaffected by both the composition and colour of the surrounding cellular medium (Mohler et al, 1996). These results were replicated in two different cell lines (LLC-MK2 and

BEAS-2B), and were further confirmed by similar results obtained using a Prestoblue cell replication assay (refer to **Supplementary Figure S2**).

We next employed a well-known commercial toxicity assay, the Lonza ToxiLight Kit, to assess cellular toxicity by measuring the levels of adenylate kinase being released into the extracellular media. Adenylate kinase is an abundant eukaryotic phosphotransferase enzyme, and upon cell death it is released into the extracellular space (Jacobs et al, 2013). Because the samples used for analysis were taken from the cellular supernantant, the cells could remain undisrupted, and cell lysis could be monitored as a function of time. The adenylate kinase detection reagent triggers a bioluminescent reaction, producing light, which could then be measured with a luminometer. $P_{220\text{-}241}$-treated cells produced the same level of bioluminescence compared to control conditions, and was markedly different from cells treated with lysis buffer, which displayed significantly more bioluminescence. Lastly, as a final measure of toxicity, a RBC lysis assay was used. Compared to the lysis buffer control, purified $P_{220\text{-}241}$ did not cause spontaneous hemolysis of RBCs. Taken together, these three assays suggest that $P_{220\text{-}241}$ is non-toxic *in vitro* when used at a concentration of 20 μM. The fact that $P_{220\text{-}241}$ is non-toxic at this micromolar concentration is unlike some other mimetics previously designed in the Mahony laboratory, such as the TRIM25 CCD mimetic produced for targeting the Influenza NS1 protein (data not shown). In contrast to the C-terminal domain of the RSV P protein, the TRIM25 CCD domain is also present in numerous other important intracellular proteins

(Choudhury et al, 2014; Pauli et al, 2014). Thus, when designing these chimeric therapeutic inhibitors, it seems important to avoid using protein domains that are already highly abundant within cells.

4.4 Mechanism of action

Following entry into cells, presumably by means of the CPP domain, we hypothesized that $P_{220-241}$ would bind to the nascent N protein and prevent its association with nascent full-length P protein. We first assessed this potential interaction using several GST pull-down assays. By using glutathione-agarose beads, we were able to bind GST-tagged proteins to these beads as bait to assess their interaction with various different prey proteins. We found that GST-tagged full-length N protein (GST-N) interacted with both $P_{220-241}$ and full-length P protein (HisNusA-P), but did not interact with either control peptides, namely HisMBP-CPP-$P_{scrambled}$ or HisNusA. Because GST-N was unable to bind to $P_{scram}$, this suggests the specificity of the N-P protein-binding interaction lies within the C-terminal 21 amino acid domain of the P protein. Furthermore, pre-incubation of GST-N with $P_{220-241}$ was able to inhibit binding of full-length P protein to GST-N, as was shown by Western blot. While informative, these pull-down results do not demonstrate unequivocally that treatment with $P_{220-241}$ is able to prevent assembly of the core polymerase complex within RSV-infected cells.

To investigate this mechanism of interaction further, we performed several co-immunoprecipitation experiments. First we demonstrated that both the N and

P proteins could co-immunoprecipitate from RSV-infected cells when using either N or P primary antibodies for the precipitation. We then showed that pre-incubation of RSV-infected LLC-MK2 cells with $P_{220-241}$ was able to disrupt the N-P interaction. Only N protein was observed to co-purify with $P_{220-241}$, while P protein was absent when probed by Western blot, as was originally expected. To the best of our knowledge, this is the first demonstration of a disruption of the essential RSV N-P interaction *in vitro* using a peptide mimetic inhibitor. Collectively, these results allow us to propose a mechanism by which $P_{220-241}$ inhibits RSV infection: the $P_{220-241}$ chimeric peptide mimetic is targeted to the cytoplasm of cells by action of the CPP, where it prevents the interaction between the nascent RSV P and N proteins, thereby preventing the formation of the essential RSV RdRp complex.

## 4.5 The continuing burden of RSV infection worldwide

Despite worldwide efforts to combat RSV infections, it continues to present a substantial global economic burden, with the costs of infections in both infants and other high-risk patients reaching into the millions of dollars (Nair et al, 2010; Paramore et al, 2004). While there have been past attempts to create safe and cost-effective treatments for RSV, there remains no vaccine, no clear-cut vaccine strategy, nor has there been any significant success with antiviral therapy (Murphy and Walsh, 1988). This presents a significant issue, considering the continuous increase in the global population, as well as the widespread

distribution of the virus. Clearly, additional novel research strategies are needed to prevent RSV infection on a global scale. Given the relative importance of the core proteins making up the RSV RdRp complex for full virulence, these various protein-protein interactions represent interesting therapeutic targets to disrupt the infection process. Additionally, a series of published studies have successfully mapped out the interaction between the RSV N and P proteins from the complex (Garcia-Barreno et al, 1996; Tran et al, 2007). Results from this study show that an RSV P protein cell-penetrating mimetic is able to successfully enter cells, bind to nascent RSV N protein, thereby inhibiting RSV infection *in vitro.* Nevertheless, while we have had success in using this strategy to target pathogens such as Chlamydia, Influenza, and RSV, there remain many challenges before a clinically useful therapeutic can be produced (discussed further below).

### 4.6.1 Future directions – binding kinetics between $P_{220-241}$ and N protein

While it was shown in this study that $P_{220-241}$ successfully binds to RSV N protein *in vitro*, we have yet to fully investigate the biochemical interaction between these two proteins. A useful variable to study in this binding relationship moving forward would be the dissociation constant ($K_D$). The $K_D$ value is an equilibrium constant which can be used to determine how readily two proteins dissociate, with smaller $K_D$ values indicating a thermodynamically favorable binding. There are several common laboratory methods that can be used to study such binding relationships, including both surface plasmon resonance (SPR) and

isothermal titration calorimetry (ITC) (Jelesaroy and Bosshard, 1999; Pattnaik, 2005). Considering the fact that other members of the Mahony laboratory are currently working on other potential RSV peptide mimetic therapeutics, it would be interesting to compare the $K_D$ values of these newer constructs to those obtained for the binding relationship between $P_{220-241}$ and the RSV N protein. Ultimately, using these methods could help in producing a therapeutic capable of binding N protein in the most thermodynamically stable fashion.

### 4.6.2 Future directions – viable human carrier molecule

In this study we utilized MBP as a molecule to help increase the solubility, and also to increase the half-life of $P_{220-241}$ by avoiding degradation. There are several theories regarding the exact mechanism by which MBP and other solubility enhancing proteins function. The most common proposition is such that these proteins help form large micelle-like aggregates, thereby shielding their passenger proteins from the surrounding solvent (Fox et al, 2001; Sachdev and Chirgwin, 1998). This process would ultimately allow the sequestered protein to achieve its native soluble conformation, provided it can spontaneously fold in the bacterial cytoplasm (Fox et al, 2001; Sachdev and Chirgwin, 1998). Thus, in order to eventually produce a viable therapeutic using the chimeric peptide mimetic strategy, their tendency to degrade and fold improperly must also be addressed for use in humans. To do this, the CPP-$P_{220-241}$ domain must be transferred to a viable human carrier molecule. Human Serum Albumin (HSA) is

an abundant human protein which has previously been shown to increase the half-life of IFN-β by approximately 4-fold (Sung et al, 2003). Previously, we successfully cloned a His-HSA-CPP-$P_{220-241}$ construct for use in the eukaryotic methylotrophic *Pichia pastoris* yeast expression system (PichiaPink$^{TM}$, Invitrogen). Unfortunately, we were not able to successfully express this construct using the system. The Mahony laboratory currently has several projects looking to address this issue. Current candidate carrier proteins being researched in the laboratory include the monocloncal Fc (mFc) domain of Immunoglobulin G (IgG), albumin-binding domain (ABD) proteins, as well as designed ankyrin repeat (DARPin) proteins, each of which have previously been described as possible carrier molecules in the scientific literature (Binz et al, 2003; Dennis et al, 2002; Ying et al, 2012).

### 4.6.3 Future directions – delivery of therapeutics

Developing an effective delivery system for these peptide mimetics will be among the most challenging roadblocks in developing an effective RSV therapeutic. Firstly, while an optimal concentration of approximately 20 μM was determined for using $P_{220-241}$ in this study, these experiments were all conducted *in vitro*. While this does provide a good initial estimate of the anti-RSV activity of this construct, it remains very plausible that a different concentration of protein would be needed for use *in vivo*. Additionally, because of the propensity for such peptides to be degraded, an efficient delivery system must be

developed. Early work has begun using probiotic bacteria to help tackle this issue. These microorganisms are generally regarded as non-pathogenic and somewhat beneficial bacteria (Fuller et al, 1991). Interestingly, many of these bacteria, such as *Lactococcus lactis* (*L. lactis*) are capable of synthesizing and then secreting proteins into the extracellular medium at mucosal sites (Bahey-El-Din et al, 2010; Morello et al, 2008). Furthermore, this delivery system has previously been employed, with considerable success, to tackle common diseases such as colon cancer (Bahey-El-Din et al, 2010). The Mahony laboratory is currently investigating several different commensals and probiotics as putative delivery vehicles. The challenge moving forward will be to develop a probiotic capable of not only colonizing the airway at sufficient levels, but which is also able to secrete a therapeutic level of desired protein.

## 4.7 Closing Remarks

RSV continues to present itself as serious pathogen worldwide, not only through infecting infants, but also the elderly and immunocompromised. There has been a continual lack of success in the development of RSV therapeutics, beginning with the disaster surrounding the formalin-innactivated vaccine during the 1960s. Currently, Palivizumab has proven to be somewhat effective in preventing RSV infection through early prophylaxis, however there remain a minimal number of useful RSV-specific antivirals. The interaction between the RSV N and P proteins presents itself as plausible therapeutic target not only due

to past studies which have mapped out their binding domains, but also because of the necessity of this interaction for full RSV virulence. Chimeric cell-penetrating peptide mimetics present themselves as novel candidates to target RSV intracellular protein-protein interactions. However, while the end goal is to eventually produce a viable *in vivo* therapeutic, there remain many hurdles that will need to be addressed. A combined effort from medical researchers around the world is crucial for helping tackle this persistent, effective, and widespread pathogen.

## References

Ahren B, Schmitz O. (2004) GLP-1 receptor agonists and DPP-4 inhibitors in the treatment of type 2 diabetes. *Horm Metab Res*. **36**, 867-876.

Ajenso A, Calvo E, Villanueva N. (2006) Phosphorylation of human respiratory syncytial virus P protein at threonine 108 controls its interaction with the M2-1 protein in the viral RNA polymerase complex. *J Gen Virol* **87**, 3637-3642.

Asenjo A, Villanueva N. (2000) Regulated but not constitutive human respiratory syncytial virus (HRSV) P protein phosphorylation is essential for oligomerization. *FEBS Lett* **467**, 279**–**284.

Arola M, Ziegler T, Ruuskanen O. (1990) Respiratory virus infection as a cause of prolonged symptoms in acute otitis media. *J Pediatr* **116**, 697-701.

Bacharier LB, Cohen R, Schweiger T, Yin-DeClue H, Christie C, Zheng J, Schechtman KB, Strunk RC, Castro M. (2012) Determinants of asthma after severe respiratory syncytial virus bronchiolitis. *J Allergy Clin Immunol* **130**, 91-100.

Bahey-El-Din M, Casey PG, Griffin BT, Gahan CG. (2010) Expression of two Listeria *monocytogenes* antigens (P60 and LLO) in *Lactococcus lactis* and examination for use as live vaccine vectors. *J Med Microbiol* **59**, 904–912.

Bangham CR, Openshaw PJ, Ball LA, King AM, Wertz GW, Askonas BA. (1986) Human and murine cytotoxic T cells specific to respiratory syncytial virus recognize the viral nucleoprotein (N), but not the major glycoprotein (G), expressed by vaccinia virus recombinants. *J Immunol* **137**, 3973-3977.

Barik S, McLean T, Dupuy LC. (1995) Phosphorylation of Ser232 directly regulates the transcriptional activity of the P protein of human respiratory syncytial virus : phosphorylation of Ser237 may play an accessory role. *Virology* **213**, 405-412.

Barry W, Cockburn F, Cornall R, Price JF, Sutherland G, Vardag A. (1986) Ribavirin aerosol for acute bronchiolitis. *Arch Dis Child* **61**, 593–597.

Batonick M, Wertz GW. (2011) Requirements for human respiratory syncytial virus glycoproteins in assembly and egress from infected cells. *Adv Virol* 2011:34308.

Baviskar PS, Hotard AL, Moore ML, Oomens AG. (2013) The respiratory syncytial virus fusion protein targets to the perimeter of inclusion bodies and facilitates filament formation by a cytoplasmic tail-dependent mechanism. *J Virol* **87**, 10730–10741.

Bawage SS, Tiwari PM, Pillai S, Dennis V, Singh SR. (2013) Recent advances in diagnosis, prevention, and treatment of human respiratory syncytial virus. *Adv Virol* **88**: 595768.

Beaucourt S and Vignuzzi M. (2014) Ribavirin: a drug active against many viruses with multiple effects on virus replication and propagation. Molecular basis of ribavirin resistance. *Curr Opinion in Virol* **8**, 10-15.

Bechara C and Sagan S. (2013) Cell-penetrating peptides: 20 years later, where do we stand? *FEBS Lett* **12**, 1693-1702.

Bermingham A, Collins PL. (1999) The M2–2 protein of human respiratory syncytial virus is a regulatory factor involved in the balance between RNA replication and transcription. *Proc Natl Acad Sci USA* **96**, 11259–11264.

Bian T, Gibbs JD, Orvell C, Imani F. (2012) Respiratory syncytial virus matrix protein induces lung epithelial cell cycle arrest through a p53 dependent pathway. *PLoS One* **7**: 38052.

Binz HK, Stumpp MT, Forrer P, Amstuz P, Puckthun A. (2003) Designing repeat proteins: well-expressed, soluble and stable proteins from combinatorial libraries of consensus ankyrin repeat proteins. *J Mol Bio* **332**, 489-503.

Bitko V, Shulyayeva O, Mazumder B, Musiyenko A, Ramaswamy M, Look DC, Barik S (2007) Nonstructural proteins of respiratory syncytial virus suppress premature apoptosis by an NFkappaB-dependent, interferon-independent mechanism and facilitate virus growth. *J Virol* **81**, 1786–1795.

Bleumink-Pluym NM, van Alphen LB, Bouwman LI, Wösten MM, van Putten JP. (2013) Identification of a functional type VI secretion system in *Campylobacter jejuni* conferring capsule polysaccharide sensitive cytotoxicity. *PLoS Pathog* **9**, 67-73.

Blondot ML, Dubosclard V, Fix J, Lassoued S, Aumont-Nicaise M, Bontems, F, Eléouët J, Sizun, C. (2012) Structure and functional analysis of the RNA- and viral phosphoprotein-binding domain of respiratory syncytial virus M2−1 protein. *PLOS Pathog* **8**: 1002734.

Blount RE Jr, Morris JA, Savage RE. (1956) Recovery of cytopathogenic agent from chimpanzees with coryza. *Proc Soc Exp Biol Med* **92**, 544–549.

Borchers AT, Chang C, Gershwin ME, Gershwin LJ. (2013) Respiratory syncytial virus—a comprehensive review. *Clin Rev Allergy Immunol* **45**, 331–379.

Brown G, Jeffree CE, McDonald T, Rixon HW, Aitken JD, Sugrue RJ. (2004) Analysis of the interaction between respiratory syncytial virus and lipid-rafts in Hep2 cells during infection. *Virology* **327**, 175–185.

Castagne N, Barbier A, Bernard J, Rezaei H, Huet JC, Henry C, Da Costa B, J. Eleouet JF. (2004) Biochemical characterization of the respiratory syncytial virus P-P and P-N protein complexes and localization of the P protein oligomerization domain. *J Gen Virol* **85**, 1643–1653.

Chang A, Dutch RE. (2012) Paramyxovirus fusion and entry: multiple paths to a common end. *Viruses* **4**, 613– 636.

Chappell KJ, Brealey JC, Mackay IM, Bletchly C, Hugenholtz P, Sloots TP and Young PR. (2013) Respiratory Syncytial Virus infection is associated with increased bacterial load in the upper respiratory tract in young children. *J Medical Microbiol Diagnosis* **S1:**005.

Chonmaitree T. (1990) Viral otitis media. *Pediatr Ann* **19**, 522-532.

Chonmaitree T, Owen MJ, Howie VM. (1990) Respiratory viruses interfere with bacteriologic response to antibiotic in children with acute otitis media. *J Infect Dis* **162**, 546-549.

Choudhury NR, Nowak JC, Zuo J, Rappsilber J, Spoel SH, Michlewski G. (2014) Trim25 is an RNA-specific activator of Lin28a/TuT4-mediated uridylation. *Cell Rep* **9**, 1265-1272.

Coates HV, Alling DW, Chanock RM. (1966) An antigenic analysis of respiratory syncytial virus isolates by a plaque reduction neutralization test. *Am J Epidemiol* **83**, 299–313.

Collins PL, Fearns R, Graham BS. (2013) Respiratory syncytial virus: virology, reverse genetics, and pathogenesis of disease. *Curr Top Microbiol Immunol* **372**, 3**–**38.

Collins PL, Hill MG, Cristina J, Grosfeld H. (1996) Transcription elongation factor of respiratory syncytial virus, a nonsegmented negative strand RNA virus. *Proc Natl Acad Sci U S A* **93**, 81–85.

Collins PL, Melero JA. (2011) Progress in understanding and controlling respiratory syncytial virus: Still crazy after all these years. *Virus Res* **162**, 80–99.

Collins PL, Mottet G. (1991) Post-translational processing and oligomerization of the fusion glycoprotein of human respiratory syncytial virus. *J Gen Virol.* **72**, 3095–3101.

Cowton VM, Fearns R. (2005) Evidence that the respiratory syncytial virus polymerase is recruited to nucleotides 1 to 11 at the 30 end of the nucleocapsid and can scan to access internal signals. *J Virol* **79**, 11311–11322.

Cowton VM, McGivern DR, Fearns R. (2006) Unravelling the complexities of respiratory syncytial virus RNA synthesis. *J Gen Virol* **87**, 1805–1821.

Crowe JE, Bui PT, Firestone CY, Connors M, Elkins WR, Chanock RM, Murphy BR. (1996) Live subgroup B respiratory syncytial virus vaccines that are attenuated, genetically stable, and immunogenic in rodents and nonhuman primates. *J Infect Dis* **173**, 829–839.

Drin G, Cottin S, Blanc E, Rees AR, Temsamani J. (2003) Studies on the internalization
mechanism of cationic cell-penetrating peptides. *J Biol Chem* **33**, 31192-31201.

Dennis MS, Zhang M, Meng YG, Kadkhodayan M, Kirchofer D, Combs D, Damico LA. (2002) Albumin binding as a general strategy for improving the pharmacokinetics of proteins. *J Biol Chem* **277**, 35035–35043.

Duttweiler L, Nadal D, Frey B. (2004) Pulmonary and systemic bacterial co-infections in severe RSV bronchiolitis. *Arch Dis Child* **89**, 1155–1157.

Enders G. (1996) Paramyxoviruses. In: Baron S (ed). *Med Microbiol* 4th ed University of Texas Medical Branch at Galveston: Galveston (TX).

Englund JA, Sullivan CJ, Jordan MC, Dehner LP, Vercellotti GM, Balfour, HH. (1988) Respiratory syncytial virus infection in immunocompromised adults. *Ann Intern Med* **109**, 203–208.

Esperante SE, Paris G, de Prat-Gay G. (2012) Modular unfolding and dissociation of the human respiratory syncytial virus phosphoprotein P and its interaction with the M2-1antiterminator: a singular tetramer-tetramer interface arrangement. *Biochemistry* **51**, 8100-8110.

Falsey AR, Hennessey PA, Formica MA, Cox C, Walsh EE. (2005) Respiratory syncytial virus infection in elderly and high-risk adults. *N Engl J Med* **352**, 1749–1759.

Fearns R, Collins PL. (1999) Model for polymerase access to the overlapped L gene of respiratory syncytial virus. *J Virol* **73**, 388–397.

Feldman SA, Audet S, Beeler JA. (2000) The fusion glycoprotein of human respiratory syncytial virus attachment and infectivity via an interaction with cellular heparin sulfate. *J Virol* **74**, 6642-6647.

Feldman SA, Hendry RM, Beeler JA. (1999) Identification of a linear heparin binding domain for human respiratory syncytial virus attachment glycoprotein G. *J Virol* **73**, 6610–6617.

Ferrari A, Pellegrini V, Arcangeli C, Fittipaldi A, Giacca M, Beltram, F. (2003) Caveolae-mediated internalization of extracellular HIV-1 tat fusion proteins visualized in real time. *Mol Ther* **8**, 284–294.

Falsey AR, Walsh EE. (2000) Respiratory syncytial virus infection in adults. *Clin Microbiol Rev* **13**, 371**–**84.

Forster A, Maertens GN, Farrell PJ, Bajorek M. (2015) Dimerization of matrix protein is required for budding of respiratory syncytial virus. *J Virol* **89**, 4624-4635.

Fox JD, Kapust RB, Waugh DS. (2001) Single amino acid substitutions on the surface of *Escherichia coli* maltose-binding protein can have a profound impact on the solubility of fusion proteins. *Protein Sci* **10**, 622–630.

Fuentes SM, Tran KC, Luthra P, Teng MN, He B. (2007) Function of the respiratory syncytial virus small hydrophobic protein. *J Virol* **81**, 8361–8366.

Fuentes SM, Sun D, Schmitt AP, He B. (2010) Phosphorylation of paramyxovirus phosphoprotein and its role in viral gene expression. *Future Microbiol* **5**, 9-13.

Fuller R. (1991) Probiotics in human medicine. *Gut* **32**, 439-442.

Galloux M, Gabiane G, Sourimant J, Richard C, England P, Moudjou M, Aumont-Nicaise M, Fix J, Rameix-Welti M, Eleouet J. (2015) Identification and characterization of the binding site of the respiratory syncytial virus phosphoprotein to RNA-Free nucleoprotein. *J Virol* **89**, 3484-3496.

Galloux M, Tarus B, Blazevic I, Fix J, Duquerroy S, Eleouet JF. (2012) Characterization of a viral phosphoprotein binding site on the surface of the respiratory syncytial nucleoprotein. *J Virol* **86**, 8375–8387.

García-Barreno B, Delgado T, Melero JA. (1996) Identification of protein regions involved in the interaction of human respiratory syncytial virus phosphoprotein and nucleoprotein: significance for nucleocapsid assembly and formation of cytoplasmic inclusions. *J Virol* **70**, 801-808.

Ghildyal R, Baulch-Brown C, Mills J, Meanger J. (2003) The matrix protein of human respiratory syncytial virus localizes to the nucleus of infected cells and inhibits transcription. *Arch Virol* **148**, 1419–1429.

Ghildyal R, Ho A, Jans DA. (2006) Central role of the respiratory syncytial virus matrix protein in infection. *FEMS Microbiol Rev* **30**, 692–705.

Ghildyal R, Jans DA, Bardin PG, Mills J. (2012) Protein-protein interactions in RSV assembly: potential targets for attenuating RSV strains. *Infect Disord Drug Targets* **12**, 103-109.

Ghildyal R, Mills J, Murray M, Vardaxis N, Meanger, J. (2002) The respiratory syncytial virus (RSV) matrix protein associates with nucleocapsids in infected cells. *J Gen Virol* **83**, 753–757.

Gonzalez PA, Bueno SM, Carreno LJ, Riedel CA, Kalergis AM. (2012) Respiratory syncytial virus infection and immunity. *Rev Medical Virol* **22**, 230–244.

Gonzalez-Reyes L, Ruiz-Arguello MB, Garcia-Barreno B, Calder L, Lopez JA, Albar JP, Skehel JJ, Wiley DC, Melero JA. (2001) Cleavage of the human respiratory syncytial virus fusion protein at two distinct sites is required for activation of membrane fusion. *Proc Natl Acad Sci USA* **98**, 9859–9864.

Giuliani A and Rinaldi AC. (2011) Beyond natural antimicrobial peptides: multimeric peptides and other peptidomimetic approaches. *Cell Mol Life Sci* **68**, 2255-2266.

Graham BS. (2011) Biological challenges and technological opportunities for respiratory syncytial virus vaccine development. *Immunol Rev* **239**, 149-166.

Hall CB. (2001) Respiratory Syncytial Virus and Parainfluenza Virus. *N Engl J Med* **344**, 1917-1928.

Hall CB, Powell KR, MacDonald NE, Gala CL, Menegus ME, Suffin SC, Cohen HJ. (1986) Respiratory syncytial viral infection in children with compromised immune function. *N Engl J Med* **315**, 77–81.

Hall CB, Simoes EA, Anderson LJ. (2013) Clinical and epidemiologic features of respiratory syncytial virus. *Curr Top Microbiol Immunol* **372**, 39-57.

Heckman KL, Pease LR. (2007) Gene splicing and mutagenesis by PCR-driven overlap extension. *Nat Protoc* **4**, 924-932.

Hendry RM, Pierik LT, McIntosh K. (1989) Prevalence of respiratory syncytial virus subgroups over six consecutive outbreaks: 1981–1987. *J Infect Dis* **160**, 185–190.

Herce HD, Garcia AE. (2007) Molecular dynamics simulations suggest a mechanism for translocation of the HIV-1 TAT peptide across lipid membranes. *Proc Natl Acad U S A* **104**, 20805-20810.

IMpact-RSV Study Group. (1998) Palivizumab, a humanized respiratory syncytial virus monoclonal antibody, reduces hospitalization from respiratory syncytial virus infection in high-risk infants. *Pediatrics* **102**, 531**–**537.

Jacobs AC, Didone L, Jobson J, Sofia MK, Krysan D, Dunman PM. (2013) Adenylate kinase release as a high-throughput-screening compatible reporter of bacterial lysis for identification of antibacterial agents. *Antimicrob Agents Chemother* **57**, 26–36.

Jelesarov I, Bosshard HR. (1999) Isothermal titration calorimetry and differential scanning calorimetry as complementary tools to investigate the energetics of biomolecular recognition. *J Mol Recognit* **12**, 3-18.

Jorquera PA, Oakley KE, Tripp RA. (2013) Advances in and the potential of vaccines for respiratory syncytial virus. *Exp Rev Respir Med* **7**, 411-427.

Kamphuis T, Meijerhof T, Stegmann T, Lederhofer J, Wilschut J, de Haan A. (2012) Immunogenicity and protective capacity of a virosomal respiratory syncytial virus vaccine adjuvanted with monophosphoryl lipid A in mice. *PLoS One* **7**:36812

Kaplan IM, Wadia JS, Dowdy SF. (2005) Cationic TAT peptide transduction domain enters cells by macropinocytosis. *J Control Release* **102**, 247–253.

Karlin D and Belshaw, R. (2012). Detecting remote sequence homology in disordered proteins: discovery of conserved motifs in the N-termini of Mononegavirales phosphoproteins. *PLoS ONE* **7**, 221-228.

Karron RA, Buonagurio DA, Georgiu AF, Whitehead SS, Adamus JE, Clements-Mann ML, Harris DO, Randolph VB, Udem SA, Murphy BR, Sidhu MS. (1997) Respiratory syncytial virus (RSV) SH and G proteins are not essential for viral replication in vitro: clinical evaluation and molecular characterization of a cold-passaged, attenuated RSV subgroup B mutant. *Proc Natl Acad Sci U S A* **94**, 13961–13966.

Kolokoltsov AA, Deniger D, Fleming EH, Roberts NJ, Karpilow JM, Davey RA. (2007) Small interfering RNA profiling reveals key role of clathrin-mediated endocytosis and early endosome formation for infection by respiratory syncytial virus. *J Virol* **81**, 7786–7800.

Kuo L, Grosfeld H, Cristina J, Hill MG, Collins PL. (1996) Effect of mutations in the gene-start and gene-end sequence motifs on transcription of monocistronic and dicistronic minigenomes of respiratory syncytial virus. *J Virol* **70**, 6892–6901.

Kwong JA, Dorfman T, Quinlan BD, Chiang JJ, Ahmed AA, Choe H, Farzan M. (2011) A tyrosine-sulfated CCR5-mimetic peptide promotes conformational transitions in the HIV-1 envelope glycoprotein. *J Virol* **15**, 7563-7571.

La Via WV, Mark MI, Stuntman HR. (1992) Respiratory syncytial virus puzzle: clinical features, pathophysiology, treatment and prevention. *J Pediatr* **121**, 503-510.

Liuzzi M, Mason SW, Cartier M, Lawetz C, McCollum RS, Dansereau N, Bolger G, Lapeyre N, Gaudette Y, Lagace L, Massariol MJ, Do F, Whitehead P, Lamarre L, Scouten E, Bordeleau J, Landry S, Rancourt J, Fazal G, Simoneau B. (2005) Inhibitors of respiratory syncytial virus replication target cotranscriptional mRNA guanylylation by viral RNA-dependent RNA polymerase. *J Virol* **79**, 13105-13115.

Llorente, MT, Garcia-Barreno B, Calero M, Camafeita E, Lopez JA, Longhi S, Ferron F, Varela PF, Melero JA. (2006) Structural analysis of the human respiratory syncytial virus phosphoprotein: characterization of an alpha-helical domain involved in oligomerization. *J Gen Virol* **87**, 159-169.

Lowry OH, Rosebrough NJ, Farr AL, Randall RJ. (1951) Protein measurement with the folin phenol reagent. *J Biol Chem* **193**, 265-275.

Lu B, Ma CH, Brazas R, Jin H. (2002). The major phosphorylation sites of the respiratory syncytial virus phosphoprotein are dispensable for virus replication in vitro. *J Virol* **76**, 10776-10784.

Martinez I, Lombardia L, Herranz C, Garcia-Barreno B, Dominguez O, Melero JA. (2009) Cultures of HEp-2 cells persistently infected by human respiratory syncytial virus differ in chemokine expression and resistance to apoptosis as compared to lytic infections of the same cell type. *Virology* **388**, 31–41.

Mason JM. (2010) Design and development of peptides and peptide mimetics as antagonists for therapeutic intervention. *Future Med Chem* **12**, 1813-1822.

Mason SW, Lawetz C, Gaudette Y, Do F, Scouten P, Lagace L, Simoneau, B, Liuzzi M. (2004) Polyadenylation-dependent screening assay for respiratory syncytial virus RNA transcriptase activity and identification of an inhibitor. *Nucleic Acids Res* **32**, 4758–4767.

Mastrangelo P, Hegele RG. (2013) RSV Fusion: Time for a New Model. *Viruses* **5**, 873-885.

Mayo MA. (1995) A listing of virus families and genera with some discriminatory features. *Arch Virol* **140**, 1337–1341.

Mazumder B, Barik, S. (1994) Requirement of casein kinase II-mediated phosphorylation for the transcriptional activity of human respiratory syncytial viral phosphoprotein P: transdominant negative phenotype of phosphorylation-defective mutant P. *Virology* **205**, 104-111.

McConnochie KM, Hall CB, Walsh EE, Roghmann KJ. (1990) Variation in severity of respiratory syncytial virus infections with subtype. *J Pediatr* **117**, 52-56.

McGivern DR, Collins PL, Fearns R (2005) Identification of internal sequences in the 30 leader region of human respiratory syncytial virus that enhance transcription and confer replication processivity. *J Virol* **79**, 2449–2460.

McGregor DP. (2008) Discovering and improving novel peptide therapeutics. *Opin Pharm* **8**, 616-619.

Mejias A, Ramilo, O. (2015) New options in the treatment of respiratory syncytial virus disease. *J Infect* **71**, 80-87.

Mitra R, Baviskar P, Duncan-Decocq RR, Patel D, Oomens AG. (2012) The human respiratory syncytial virus matrix protein is required for maturation of viral filaments. *J Virol* **86**, 4432–4443.

Mohler WA, Charlton CA, Blau HM. (1996) Spectrophotometric quantitation of tissue culture cell number in any medium. *Biotechniques* **21**, 264-266.

Morello E, Bermudez-Humaran LG, Llull D, Sole V, Miraglio N, Langella P, Poquet L. *Lactococcus lactis*, an efficient cell factory for recombinant protein production and secretion. *J Mol Microbiol Biotechnol* **14**, 48-58.

Mufson MA, Orvell C, Rafnar B, Norrby E. (1985) Two distinct subtypes of human respiratory syncytial virus. *J Gen Virol* **66**, 2111–2124.

Murata, Y. (2009) Respiratory syncytial virus vaccine development. *Clin Lab Med* **29**, 725**–**739.

Murray J, Loney C, Murphy LB, Graham S, Yeo RP. (2001) Characterization of monoclonal antibodies raised against recombinant respiratory syncytial virus nucleocapsid (N) protein: identification of a region in the carboxy terminus of N involved in the interaction with P protein. *Virology* **289**, 252-261.

Murray J, Saxena S and Sharland M. (2014) Preventing severe respiratory syncytial virus disease: passive, active immunisation and new antivirals. *Arch Dis Child* 99, 469-473.

Murphy BR and Walsh EE. (1988) Formalin-inactivated respiratory syncytial virus vaccine induces antibodies to the fusion glycoprotein that are deficient in fusion-inhibiting activity. *J Clin Microbiol* **26**, 1595-1597.

Nair H, Nokes D, Gessner B, Dherani M, Madhi S, Singleton R, O'Brien K, Roca A, Wright P, Bruce N, Chandran A, Theodoratou E, Sutanto A, Sedyaningsih E, Ngama M, Munywoki P, Kartasasmita C, Simoes E, Rudan I, Weber M, Campbell H. (2010) Global burden of acute lower respiratory infections due to respiratory syncytial virus in young children: a systematic review and meta-analysis. *The Lancet* **375**, 1545-1555.

Nair H, Verma VR, Theodoratou E, Zgaga L, Huda T, Simoes EA, Wright PF, Rudan I, Campbell H. (2011) An evaluation of the emerging interventions against Respiratory Syncytial Virus (RSV)-associated acute lower respiratory infections in children. *BMC Publ Health* **11**, 1-16.

Nallamsetty S, Waugh DS. (2006). Solubility enhancing proteins MBP and NusA play a passive role in the folding of their fusion partners. *Protein Expr Purif* **45**, 175**–**182.

Navarro J, Lopez-Otin C, Villanueva N. (1991) Location of phosphorylated residues in human respiratory syncytial virus phosphoprotein. *J Gen Virol* **72**, 1455–1459.

Ogra PI. (2004) Respiratory syncytial virus: the virus, the disease and the immune response. *Paediatr Respir Rev* **5** (Suppl. A):S119–S126.

Oliveira AP, Simabuco FM, Tamura RE, Guerrero MC, Ribeiro PG, Libermann TA, Zerbini LF, Ventura AM. (2013) Human respiratory syncytial virus N, P and M protein interactions in HEK-293T cells. *Virus Res* **177**, 108-12

Olson GL, Bolin DR, Bonner MP, Bo¨s M, Cook CM, Fry DC, Graves BJ, Hatada M, Hill DE, Kahn M, Madison VS, Rusiecki VK, Sarabu R, Sepinwall J, Vincent GP, Voss ME. (1993) Concepts and progress in the development of peptide mimetics. *J Med Chem* **36**, 3039**-**3049.

Paes BA, Mitchell I, Banerji A, Lanctot KL, Langley JM. (2011) A decade of respiratory syncytial virus epidemiology and prophylaxis: translating evidence into everyday clinical practice. *Can Respir J* **18**, 10–19.

Panozzo CA, Fowlkes AL, Anderson LJ. (2007) Variation in timing of respiratory syncytial virus outbreaks: lessons from national surveillance. *Pediatr Infect Dis J* **26**, 41–45.

Papadopoulos NG, Gourgiotis D, Javadyan A, Bossios A, Kallergi K, Psarras S, Tsolia MN, Kafetzis D. (2004) Does respiratory syncytial virus subtype influences the severity of acute bronchiolitis in hospitalized infants? *Respir Med* **98**, 879–882.

Paramore LC, Ciuryla V, Ciesla G, Liu L. (2004) Economic impact of respiratory syncytial virus-related illness in the US: an analysis of national databases. *Pharmacoeconomics* **22**, 275-284.

Pastey, MK, Crowe JE, Braham BS. (1999) RhoA interacts with the fusion glycoprotein of respiratory syncytial virus and facilitates virus-induced syncytium formation. *J Virol* **73**, 7262–7270.

Pattnaik P. (2005) Surface plasmon resonance: applications in understanding receptor-ligand interaction. *Appl Biochem Biotechnol* **126**, 79-92.

Pauli EK, Chan YK, Davis ME, Gableske S, Wang MK, Feister KF, Gack MU. (2014) The ubiquitin-specific protease USP15 promotes RIG-I mediated antiviral signaling by deubiquitylating TRIM25. *Sci Signal* **7**:ra3

Polack FP, Teng MN, Collins PL, Prince GA, Exner M, Regele H, Lirman DD, Rabold R, Hoffman SJ, Karp CL, Kleeberger SR, Wills-Karp M, Karron RA. (2002) A role for immune complexes in enhanced respiratory syncytial virus disease. *J Exp Med* **196**, 859**–**865.

Prince GA, Curtis SJ, Yim KC, Porter DD. (2001) Vaccine enhanced respiratory syncytial virus disease in cotton rats following immunization with Lot 100 or a newly prepared reference vaccine. *J Gen Virol* **82**, 2881**–**2888.

Pullan CR, Hey EN. (1982) Wheezing, asthma and pulmonary dysfunction 10 years after infection with respiratory syncytial virus. *BMJ* **284**, 1665–1669.

Randolph AG, Reder L, Englund JA. (2004) Risk of bacterial infection in previously healthy respiratory syncytial virus-infected young children admitted to the intensive care unit. *Pediatr Infect Dis J* **23**, 990–994.

Richard JP, Melikov K, Vives E, Ramos C, Verbeure B, Gait MJ, Chernomordik LV, Lebleu B. (2003) Cell-penetrating peptides. A reevaluation of the mechanism of cellular uptake. *J Chem Bio* **278**, 585-590.

Rodriguez R, Ramilo O. (2014) Respiratory syncytial virus: How, why and what to do. *J Infect* **68**, 115-118.

Rudraraju R, Jones B, Sealy R, Surman S, Hurwitz J. (2013) Respiratory Syncytial Virus: Current Progress in Vaccine Development. *Viruses* **5**, 577–594.

Saalik P, Elmquist A, Hansen M, Padari K, Saar K, Viht K, Langel U, Pooga M. (2004) Protein cargo delivery properties of cell-penetrating peptides. A comparative study. *Bioconjugate Chem* **15**, 1246–1253.

Sachdev D, Chirgwin JM. (1998) Order of fusions between bacterial and mammalian proteins can determine solubility in Escherichia coli. *Biochem Biophys Res Commun* **244**, 933–937.

Samal SK. (2011) Newcastle disease and related avian paramyxoviruses, p 69–114. In Samal SK (ed), The biology of paramyxoviruses. Caister Academic Press, Norfolk, United Kingdom.

Sastre P, Ruiz T, Schildgen O, Vela C, Rueda P. (2012) Seroprevalence of human respiratory syncytial virus and human metapneumovirus in healthy population analyzed by recombinant fusion protein-based enzyme linked immunosorbent assay. *J Virol* **9**, 1-5.

Schickli JH, Dubovsky F, Tang RS. (2009) Challenges in developing a pediatric RSV vaccine. *Hum Vaccin* **5**, 582**–**591.

Sigurs, N, Bjarnason R, Sigurbergsson F, Kjellman B, Björkstén B. (1995) Asthma and immunoglobulin E antibodies after respiratory syncytial virus bronchiolitis: a prospective cohort study withmatched control subjects. *Pediatrics* **95**, 500–505.

Sigurs N, Bjarnason R, Sigurbergsson F, Kjellman B. (2000) Respiratory syncytial virus bronchiolitis in infancy is an important risk factor for asthma and allergy at age 7. *Am J Respir Crit Care Med* **161**,1501-1507.

Sonne DP, Engstrom T, Treiman M. (2008) Protective effects of GLP-1 analogues exendin-4 and GLP-1(9-36) amide against ischemia-reperfusion injury in rat heart. *Reg Pept* **146**, 243-249.

Sourimant J, Rameix-Welti M, Gaillard A, Chevret D, Galloux M, Gault E, Eleouet J. (2015) Fine mapping and characterization of the L-polymerase-binding domain of the respiratory syncytial virus phosphoprotein. *J Virol* **89**, 4421-4433.

Spann KM, Tran KC, Chi B, Rabin RL, Collins PL. (2004) Suppression of the induction of α, β, and γ interferons by the NS1 and NS2 proteins of human respiratory syncytial virus in human epithelial cells and macrophages. *J Virol* **78**, 4363–4369.

Spann KM, Tran KC, Collins PL. (2005) Effects of nonstructural proteins NS1 and NS2 of human respiratory syncytial virus on interferon regulatory factor 3, NF-κB, and proinflammatory cytokines. *J Virol* **79**, 5353–5362.

Stenballe LG, Drvasundaram JK, Simoes EA. (2003) Respiratory syncytial virus epidemics: the ups and downs of a seasonal virus. *Pediatr Infect Dis J* **22**, 21-32.

Stone CB, Bulir DC, Emdin CA, Pirie RM, Porfilio EA, Slootstra JW, Mahony JB. (2011) *Chlamydia pneumoniae* CdsL regulates CdsN ATPase activity, and disruption with a peptide mimetic prevents bacterial invasion. *Front Microbiol* **2**, 21.

Sullender WM. (2000) Respiratory syncytial virus genetic and antigenic diversity. *Clin Microbiol Rev* **13**, 1–15.

Sung C, Nardelli B, LaFleur DW, Blatter E, Corcoran M, Olsen HS, Birse CE, Pickeral OK, Zhang J, Shah D, Moody G, Gentz S, Beebe L, Moore PA. (2003) An IFN-beta-albumin fusion protein that displays improved pharmacokinetic and pharmacodynamic properties in nonhuman primates. *J Interferon cytokin Res* **23**, 25-36.

Tang YW, Graham BS. (1994) Anti-IL-4 treatment at immunization modulates cytokine expression, reduces illness, and increases cytotoxic T lymphocyte activity in mice challenged with respiratory syncytial virus. *J Clin Invest* **94**, 1953-1958.

Tayyari F, Marchant D, Moraes T, Duan W, Mastrangelo P and Hegele RG. (2011) Identification of nucleolin as a cellular receptor for human respiratory syncytial virus. *Nature* **17,** 1132-1135.

Tawar G, Duquerroy S, Vonrhein C, Varela PF, Damier-Piolle L, MacLellan K, Bedouelle H, Bricogne H, Bhella D, Eleouet JF, Rey FA. (2009) Crystal structure of a nucleocapsid-like nucleoprotein-RNA complex of respiratory syncytial virus. *Science* **326**, 1279-1283.

Ter-Avetisyan G, Tunnemann G, Nowak D, Nitschke M, Herrmann A, Drab M, Cardoso MC. (2009) Cell entry of arginine-rich peptides is independent of endocytosis. *J Biol Chem* **284**, 3370–3378.

Thompson WW, Shay DK, Weintraub E, Brammer L, Cox N, Anderson LJ, Fukuda K. (2003) Mortality associated with influenza and respiratory syncytial virus in the United States. *JAMA* **289**, 179-86.

Thorburn K, Harigopal S, Reddy V, Taylor N, van Saene HKF. (2006) High incidence of pulmonary bacterial co-infection in children with severe respiratory syncytial virus (RSV) bronchiolitis. *Thorax* **61**, 611–615.

Tran TL, Castagne N, Bhella D, Varela PF, Bernard J, Chilmonczyk S, Berkenkamp S, Benhamo V, Grznarova K, Grosclaude J, Nespoulos C, Rey FA, Eleouet JF. (2007) The nine C-terminal amino acids of the respiratory syncytial virus P are necessary and sufficient for binding to ribonucleoprotein complexes in which six ribonucleotides are contacted per N protein protomer. *J Gen Virol* **88**, 196–206.

Turner TL, Kopp BT, Paul G, Landgrave LC, Hayes D Jr, Thompson R. (2014) Respiratory syncytial virus: current and emerging treatment options. *Clinicoecon Outcomes Res* **6**, 217-225.

Utley TJ, Ducharme NA, Varthakavi V, Shepherd BE, Santangelo PJ, Lindquist ME, Goldenring JR, Crowe Jr JE. (2008) Respiratory syncytial virus uses a Vps4-independent budding mechanism controlled by Rab11-FIP2. *Proc Natl Acad Sci U S A* **105**, 10209**–**10214.

Villanueva N, Hardy R, Asenjo A, Yu Q, Wertz, G. (2000) The bulk of the phosphorylation of human respiratory syncytial virus phosphoprotein is not essential but modulates viral RNA transcription and replication. *J Gen Virol* **81**, 129–133.

Villanueva N, Navarro J, Cubero E. (1991) Antiviral effects of xanthate D609 on the human respiratory syncytial virus growth cycle. *Virology* **181**, 101-108.

Walsh EE, Falsey AR. (2012) Respiratory syncytial virus infection in adults. *Infect Disord Drug Targets* **12**, 98-102.

Walsh EE, Hruska J. (1983) Monoclonal antibodies to respiratory syncytial virus proteins: identification of the fusion protein. *J Virol* **47**, 171-177.

Welliver RC. (2003) Review of epidemiology and clinical risk factors for severe respiratory syncytial virus (RSV) infection. *J Pediatr* **143**, 112–117.

Werle M, Bernkop-Schnurch A. (2006) Strategies to improve plasma half life time of peptide and protein drugs. *Amino Acids* **30**, 351-367.

Wright M, Piedimonte G. (2011) Respiratory syncytial virus prevention and therapy: past, present, and future. *Pediatr Pulmonol* **46**, 324–347.

Ying T, Chen W, Gong R, Feng Y, Dimitrov DS. (2012) Soluble Monomeric IgG1 Fc. *J Biol Chem* **287**, 19399-19408.

Yu Q, Davis PJ, Barrett T, Binns MM, Boursnell ME, Cavanagh D. (1991) Deduced amino acid sequence of the fusion glycoprotein of turkey rhinotracheitis virus has greater identity with that of human respiratory syncytial virus, a pneumovirus, than that of paramyxoviruses and morbilliviruses. *J Gen Virol* **72**, 75–81.

Yu Q, Hardy RW, Wertz GW. (1995) Functional cDNA clones of the human respiratory syncytial (RS) virus N, P, and L proteins support replication of RS virus genomic RNA analogs and define minimal trans-acting requirements for RNA replication. *J Virol* **69**,2412–2419.

Zeng R, Cui Y, Hai Y, Liu Y. (2012) Pattern recognition receptors for respiratory syncytial virus infection and design of vaccines. *Virus Res* **167**, 138**–**145.

Zhou H, Thompson WW, Viboud CG, Ringholz CM, Cheng P, Steiner C, Abedi GR, Anderson LJ, Brammer L, Shay DK. (2012) Hospitalizations associated with influenza and respiratory syncytial virus in the United States, 1993-2008. *Clin Infect Dis* **54**, 1427-1436.

# APPENDIX

## 5.1 Supplementary Figures

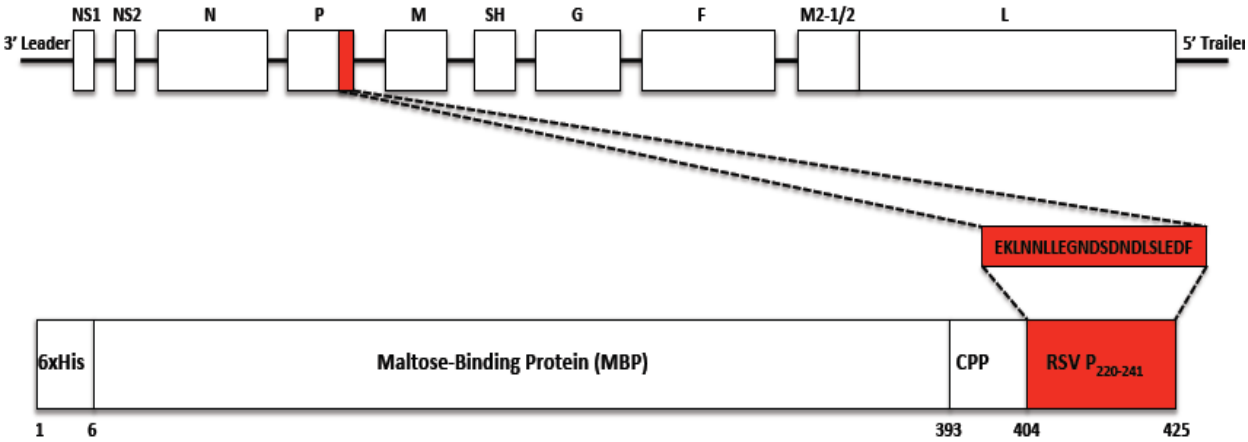


**Supplementary Figure S1. Schematic overview of $P_{220-241}$ construct design.**
The final 21 C-terminal amino acids of RSV P were linked to a cell-penetrating peptide (CPP), Maltose-Binding Protein (MBP), and a polyhistidine tag for purification and detection. The construct is depicted from left (N-terminus) to right (C-terminus). The final chimeric protein is 425 amino acids in length and has a molecular weight of approximately 47 kDa.

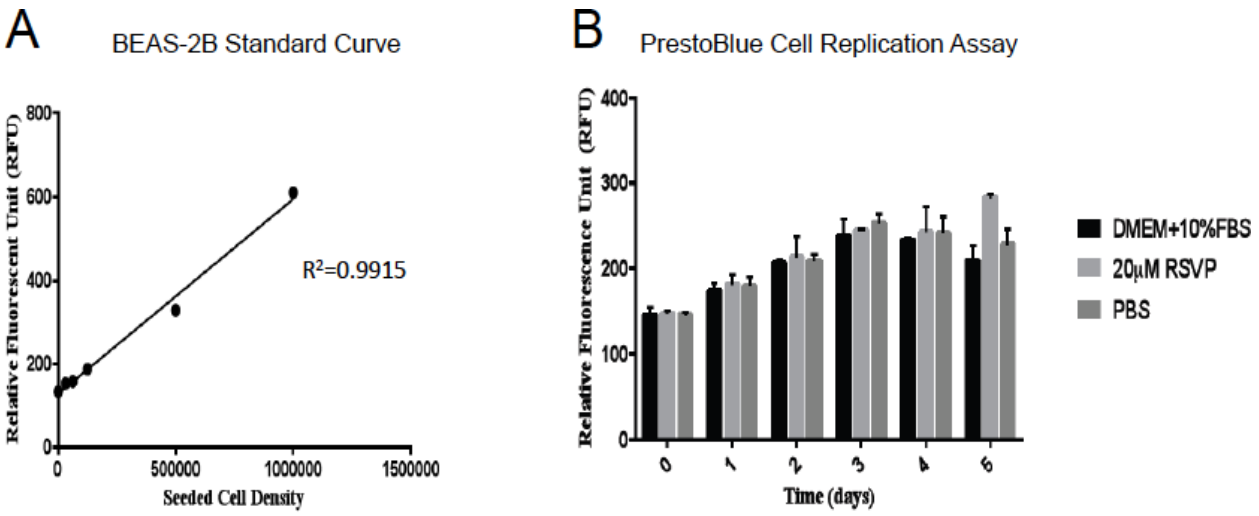


**Supplementary Figure S2. $P_{220-241}$ does not inhibit cell replication (PrestoBlue Assay)**
**(A)** BEAS-2B cells were seeded at different cell densities by serial dilution before being incubated with PrestoBlue reagent. RFU measurements were then made, and linear regression analysis was performed. The equation for the line of best fit was (0.0004679±0.00002172)x+(127.6±9.996) and the coefficient of determination, $R^2$, was 0.9915. **(B)** BEAS-2B cells were seeded in 24-well plates and treated with one of the following conditions: DMEM+10% FBS, PBS in DMEM+10% FBS, or $P_{220-241}$ (20 μM). At the appropriate time point, the cells were incubated with PrestoBlue reagent, and RFU measurements were taken (excitation wavelength: 535 nm; emission wavelength 615 nm). Error bars represent standard deviation from the mean of 3 independent experiments.

5.2 Supplementary Tables

| **Bacterial Strain** | **Plasmid** | **Insert Gene** | **Protein Construct** | **Antibiotic Resistance** |
|---|---|---|---|---|
| *E. coli* BL21 (DE3) | pDESTHisMBP | $P_{220-241}$ | HisMBP-NLS-$P_{220-241}$ | Ampicillin |
| *E. coli* BL21 (DE3) | pDESTHisMBP | $P_{scram}$ | HisMBP-NLS-$P_{scram}$ | Ampicillin |
| *E. coli* BL21 (DE3) | pDESTHisMBP | PB1 T6R | HisMBP-NLS-PB1 T6R | Ampicillin |
| *E. coli* BL21 (DE3) | pDEST15 (GST-tag) | none | GST | Ampicillin |
| *E. coli* BL21 (DE3) | pDEST15 (GST-tag) | N | GST-N | Ampicillin |
| *E. coli* Rosetta (DE3) | pDEST544 (HisNusA-tag) | P | HisNusA-P | Ampicillin |
| *E. coli* BL21 (DE3) | pDEST544 (HisNusA-tag) | none | HisNusA | Ampicillin |

**Table 5.1 – List of *E. coli* expression strains**

Please note that ampicillin was used a working concentration of 100 µg/mL.

| RSV A Strain | Sequence | RSV B Strain | Sequence |
|---|---|---|---|
| USA/79E-495-01/1979 | EKLNNLLEGNDSDNDLSLEDF | USA/98I-010A-01/1998 | KKLSDLLEDNDSDNDLSLDDF |
| MEX/59/2007 | EKLNNLLEGNDSDNDLSLEDF | USA/91I-020A-01 | KKLSDLLEDNDSDNDLSLDDF |
| USA/LA2_56/2013 | EKLNNLLEGNDSDNDLSLEDF | USA/LA2_51/2013 | KKLSDLLEDNDSDNDLSLDDF |

**Table 5.2 – Amino acid sequences of the C-terminal 21 amino acids of P in RSV A/B**

Note: Black amino acids represent those which are identical between all strains of RSV A and B. Amino acids coloured in red represent those in RSV B which are different from those in RSV A.